

Copyright
by
Marcus André de Carvalho Torres
2008

The Dissertation Committee for Marcus André de Carvalho Torres
certifies that this is the approved version of the following dissertation:

Topics in Metastable Supersymmetry Breaking

Committee:

Vadim Kaplunovsky, Supervisor

Jacques Distler

Willy Fischler

Dan Freed

Sonia Paban

Topics in Metastable Supersymmetry Breaking

by

Marcus André de Carvalho Torres, B.S., M.Sc.

DISSERTATION

Presented to the Faculty of the Graduate School of
The University of Texas at Austin
in Partial Fulfillment
of the Requirements
for the Degree of

DOCTOR OF PHILOSOPHY

THE UNIVERSITY OF TEXAS AT AUSTIN

May 2008

Dedicated to my parents Janilde and Paulo, brothers Fabius and Marco Paulo, aunties Jaine, Lulu, Elba, Vera, Denise, Elma and Janilce. Thanks for all the support, for enduring the distance and keeping me in your hearts.

Acknowledgments

I wish to thank the multitudes of people who helped me. Vadim Kaplunovsky was a superb advisor, paying attention at each step of my intellectual progress, with lot of patience. Sonia Paban, Willy Fischler and Steven Weinberg and Vadim taught me excellent classes, and Jacques Distler always brought clever insights in our group discussion and incentivated me to give talks in the Geometry/Strings seminars as soon as I came to Austin. I thank my colleagues in the group, in the brazilian/latino community in Austin and my very best friends Dolgor, Nacho, Mauricio, Ricardo, Velma, Donald, Amy, Lula and Sergio.

Topics in Metastable Supersymmetry Breaking

Publication No. _____

Marcus André de Carvalho Torres, Ph.D.
The University of Texas at Austin, 2008

Supervisor: Vadim Kaplunovsky

Supersymmetry helps simplifying the hierarchy problem, it provides candidates for dark matter and it leads to the desirable gauge coupling unification. Nevertheless, Supersymmetry is not found around us, and it has to be a broken symmetry. In this thesis we explore a different paradigm where supersymmetry is not broken in the true vacuum. Instead we live in a long living meta-stable vacuum that is not supersymmetric.

Table of Contents

| | |
|---|-----------|
| Acknowledgments | v |
| Abstract | vi |
| List of Tables | ix |
| List of Figures | x |
| Chapter 1. Introduction | 1 |
| Chapter 2. The ISS Model | 6 |
| 2.1 Supersymmetry-breaking sector | 6 |
| 2.2 Dynamical Supersymmetry Restoration | 9 |
| 2.3 Metastable vacuum decay | 10 |
| Chapter 3. Cosmological History of Metastable Supersymmetry Breaking | 18 |
| 3.1 Free Energy | 21 |
| 3.1.1 Mass Matrices in the Meson Directions | 22 |
| 3.1.2 Mass Matrices in the Quark Directions | 23 |
| 3.1.3 Effective potential | 28 |
| 3.2 Cooling and the Emergence of Different Phases | 31 |
| Chapter 4. Flavor Gauging | 42 |
| 4.1 Numerical Evaluation of CW Potential | 45 |
| 4.2 Renormalization Group Equations | 46 |
| 4.3 Phase Structure | 49 |
| 4.4 Results | 51 |
| 4.5 Generic Moduli Space | 51 |

| | |
|------------------------------------|----|
| Chapter 5. Conclusion | 54 |
| Appendix | 57 |
| Appendix 1. Triangle Approximation | 58 |
| Bibliography | 62 |
| Vita | 66 |

List of Tables

| | | |
|-----|---|----|
| 3.1 | fermions masses, meson direction | 23 |
| 3.2 | real scalar squared masses, meson direction | 24 |
| 3.3 | real scalar squared masses, sectors 2 and 3 | 26 |
| 3.4 | vector boson and fermion masses, sector 4 | 28 |
| 3.5 | real squared masses for bosons, sector 4 | 29 |

List of Figures

| | | |
|-----|---|----|
| 2.1 | Schematic vacuum structure of zero-temperature theory | 9 |
| 2.2 | Classical potential from Metastable vacuum to SUSY vacuum | 14 |
| 2.3 | Classical potential in bounce path | 15 |
| 2.4 | ISS and hump free bounce paths in 3D field space | 16 |
| 2.5 | Potential along the bounce path with moduli lifted | 17 |
| 3.1 | Evolution of the effective potential with temperature | 39 |
| 3.2 | Free energy in squark direction at different temperatures. $T_1^Q >$ $T_2^Q = T_c^Q$ | 40 |
| 3.3 | Effective potential for every values of ϕ and Q for $T \sim T_c^Q$. . | 41 |
| 4.1 | φ_{min} versus $\mathbb{R}/2 = g_f^2/2h^2$ | 46 |
| 4.2 | Effective potential for different values of \mathbb{R} | 47 |
| 4.3 | τ versus ν | 52 |
| 4.4 | Minimum of potential at $\mathbb{R} = 0.25$ | 53 |
| 1.1 | Potential before and after triangle approximation | 61 |

Chapter 1

Introduction

The idea of breaking Supersymmetry in a meta-stable vacuum is an old one [13, 16], but only recently it became the focus of investigation. In part, I believe it is due to a change of perspective on Supersymmetry Breaking and String Theory. In the last five years, it became more acceptable that our Universe may not be the single solution dictated by the dynamics of String Theory, but there is a ocean, or a Landscape [28], of solutions where the one we live was randomly selected. In this mindset, It was also natural to presume that an effective supersymmetric model could have several vacuum solutions, some supersymmetric and others non-supersymmetric, with positive energy. Naturally, we can only live in such meta-stable vacuum if its tunneling rate is exponentially suppressed, with a half-life bigger than the age of our Universe.

There are reasons to believe we live in a meta-stable vacuum [21], especially when considering models without gravity. A condition for Supersymmetry breaking in generic¹ models is the existence of a continuous $U(1)_R$ global symmetry [25]. This symmetry must be spontaneously broken in order to allow

¹Generic models are such in which all terms consistent with the symmetries of the model are present and gauge interactions are not in strong regime [25].

gaugino mass terms and such breaking would lead to the existence of a massless Goldstone Boson, R-axion. Phenomenologically, a massless R-axion is ruled out. Therefore, it is necessary that R-symmetry be only an approximate symmetry. In this circumstance we can only have metastable supersymmetry breaking.

In theories that consider gravity [6], for each generic model it is possible to create a nongeneric model that preserves the Supersymmetry breaking mechanism adding a constant term to the superpotential that breaks R-symmetry explicitly, desirably suppress the cosmological constant and generates mass to the R-axion. There is no contradiction with the statements in [25] because genericity is not respected in these models. Nevertheless such gravity models do not explain the origin of the constant term in the superpotential and the fine tuning of the cosmological constant. Therefore it is still attractive to consider generic models with approximate R-symmetry for metastable Supersymmetry breaking and search for other appropriate solutions for the fine tuning of the Cosmological Constant.

Spontaneous Supersymmetry breaking (metastable or not) has some challenges in order to describe a real world physics. The mass squared sum rule

$$S\text{Tr}(m^2) = \sum_j (-1)^{2j} (2j+1) \text{Tr}(m_j^2) = 0 \quad (1.1)$$

shows that F-term and D-term Supersymmetry breaking preserve the mass squared traces of fermions and bosons in the chiral multiplets. If the Supersymmetry breaking occurred directly in the Standard Model (in its supersym-

metric version), we should already be able to see the supersymmetric partners of quarks and leptons. Hence, Supersymmetry must be broken in a separate hidden sector and be mediated to the Standard Model Sector. Several mediation mechanisms are understood today, mainly gravity mediation, anomaly mediation and gauge mediation [18].

Another concern is related to the mass hierarchy problem. The Higgs mass is believed to be of the order of the Electroweak Scale m_W but 1-loop calculation gives a quadratic divergent correction to the tree level mass of the Higgs boson. The divergence stops at the cutoff scale given by the Supersymmetry breaking scale M_{SB} once fermionic loops start canceling the scalar loops at energies above M_{SB} . If M_{SB} is much bigger than m_W , an unnatural fine tuning would have to take place to bring the Higgs mass close to m_W . Furthermore, Supersymmetry, or a supersymmetric version of the Standard Model, is an effective theory and it is believed to have one single natural scale M_S related to the phase transition from a more fundamental theory. Within the context of gauge Unification, M_S is expected to be close to the unification scale of 10^{16}GeV . The natural way to avoid a fine tuning of the order of 10^{-14} in the Higgs mass, is the dynamical generation of a lower scale (dimensional transmutation) in gauge theories:

$$\Lambda = e^{-8\pi^2/bg^2(M_S)} M_S \quad (1.2)$$

In 2006, Intriligator, Seiberg and Shih built a model [20] of metastable supersymmetry breaking (MSB) that not only has the attractive dynamically

generated scale that improves the mass hierarchy problem but also it has a dynamical Supersymmetry restoration, that keeps the true vacuum far away from the metastable vacuum, giving longevity to the metastable vacuum. Such model is not suitable to describe QCD or Standard Model physics since it has no chiral symmetry breaking and it is IR free, but it is a good candidate to a MSB hidden sector of a theory that contains the Standard Model[2, 3, 5, 32].

A few concerns remained to be analyzed in this model. In the context of real world physics, it is fair to ask if the time evolution of our Universe would bring us to the metastable vacuum or if it would takes directly to the stable supersymmetric vacuum. If the last were the case, Supersymmetry would never be broken. Our studies in a pos-inflationary era provide some hints that the cosmological evolution favors the MSB vacuum as we show in chapter 3.

Another interesting issue is in reference to flavor symmetry. A gauge mediation mechanism is realized by gauging the flavor symmetry or part of it. Gauging the flavor symmetry can possibly endanger the vacuum metastability by shifting the false vacuum closer to the absolute vacuum through inverse hierarchy [8, 30]. We were able to show that with few assumptions on the natural scales of the flavor and color gauge symmetries, the metastable vacuum remains long living.

In chapter 2 we lay the ISS model out. In chapter 3, we study the cosmological history of the ISS model. In chapter 4 we gauge the flavor symmetry and in chapter 5 we conclude this dissertation putting the subject in

perspective within particle physics and tracing our future steps on the subject.

Chapter 2

The ISS Model

In 2006 Intriligator, Seiberg and Shih introduced a model (ISS) [20] of meta-stable supersymmetry breaking using Seiberg's electromagnetic duality [27] characteristic of QCD like supersymmetric models. The magnetic phase, would be a $SU(N)$ SQCD with large number of flavors $N_f > 3N$ and extra flavor bifundamentals, color-invariant. The bifundamental fields are relic meson fields of the UV completion, the electric phase. The electric phase continues to have the same number of flavors N_f and $N_f - N$ colors and it is therefore UV free. Our interest is in the IR free magnetic phase. Its Witten Index [31] is N and therefore it has N supersymmetric vacua, but Intriligator, Seiberg and Shih were able to show the existence of a meta-stable, non-supersymmetric vacuum far away from the supersymmetric vacua in the field configuration space.

2.1 Supersymmetry-breaking sector

The meta-stable susy breaking vacuum is in a region of field space near the origin, where non-perturbative effects are negligible. In this region, a O' Raifeartaigh spontaneous supersymmetry breaking mechanism [26] takes

place. The superpotential for the theory (including the non-perturbative piece arising from gaugino condensation) is,

$$W = h \text{Tr } q\Phi\tilde{q} - h\mu^2 \text{Tr}\Phi + AN(\det\Phi)^{1/N} \quad (2.1)$$

where

$$A \equiv h^\nu \Lambda_m^{-\nu+3}, \quad \nu = N_f/N. \quad (2.2)$$

In our notation, the q stand for the (dual) quarks, the Φ are gauge singlet mesons and Λ_m is the dynamically generated scale (the scale of the Landau pole) for the IR theory. In the presence of the second term, a $SU(N_f)^2$ flavor symmetry is broken into a diagonal $SU(N_f)$ and the bifundamentals Φ split into a singlet and a flavor adjoint. The matter content can be described by (the columns denote the $SU(N)$ gauge and global symmetry groups):

| | $SU(N)$ | $SU(N_f)$ | $U(1)_B$ | $U(1)_R$ |
|-------------|----------------|------------------|----------|----------|
| Φ_a | 1 | $(N_f^2 - 1)$ | 0 | 2 |
| Φ_I | 1 | 1 | 0 | 2 |
| q | N | $\overline{N_f}$ | 1 | 0 |
| \tilde{q} | \overline{N} | N_f | -1 | 0 |

The number of colors of the magnetic theory N , and the number of flavors N_f , satisfy $N_f > 3N$ so that the theory is IR free. In this picture, R-symmetry is anomalous, but in the weak coupling limit of IR, $SU(N)$ gauge symmetry approximates to a flavor symmetry and R-symmetry becomes an approximate symmetry which satisfy a general condition for supersymmetry breaking [25].

For small meson fields, the non-perturbative term can be dropped, and we can calculate the moduli space of susy-breaking tree-level vacua. These are at

$$\langle \Phi \rangle = \begin{pmatrix} 0 & 0 \\ 0 & \varphi \end{pmatrix}, \quad \langle q \rangle = \begin{pmatrix} Q \\ 0 \end{pmatrix}, \quad \langle \tilde{q} \rangle = (\tilde{Q} \quad 0), \quad (2.3)$$

with $\tilde{Q}Q = \mu^2 \mathbb{I}_N$ where \tilde{Q} and Q are $N \times N$ matrices and φ is a $(N_f - N) \times (N_f - N)$ matrix. In this vacuum the scalar potential has the value

$$V_{min} = (N_f - N)|h^2\mu^4|$$

The point of maximum global symmetry in this moduli space, up to gauge transformation and flavor rotation, is

$$\varphi = 0, \quad Q = \tilde{Q} = \mu \mathbb{I}_N, \quad (2.4)$$

The interesting point is that along with these meta-stable vacua, far away in the moduli-space at large meson values, we have supersymmetric vacua that arise from the extremization of the superpotential. These are of course the familiar SUSY vacua of SYM.

Putting all these together, the vacuum structure of the IR dual of SQCD looks schematically like Fig. 2.1. The susy-breaking vacuum is in a local trough (in all directions, even though we indicate only the quark direction), so it is meta-stable and it is cosmologically stable due to a large potential barrier. At the tree level, there is one special direction where the potential remains flat, but 1-loop corrections raise a potential barrier. We will further comment on this on section 2.3.

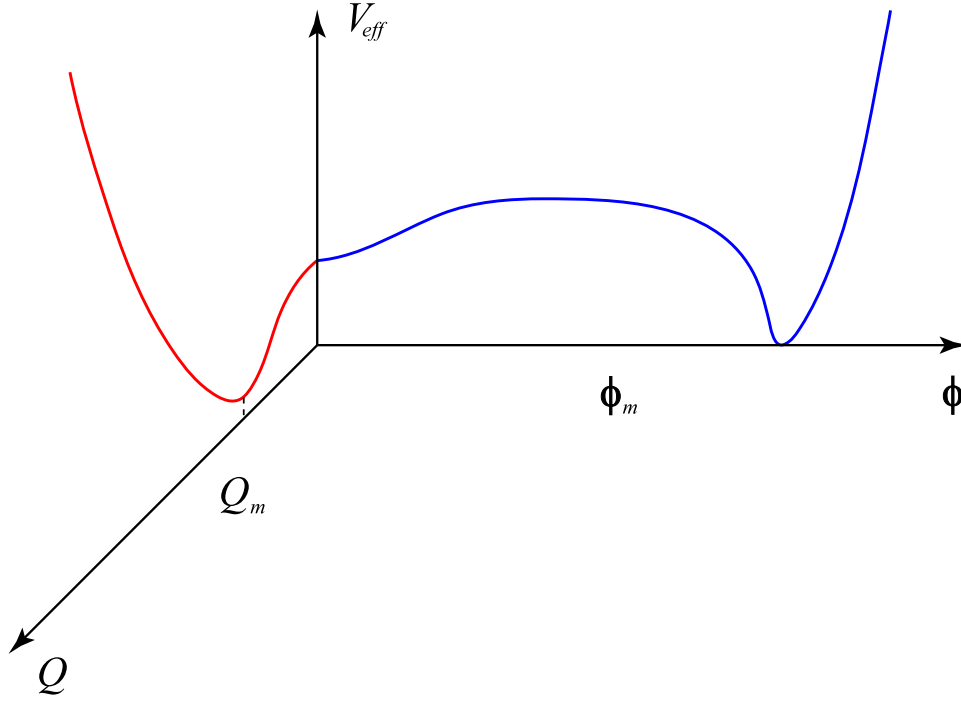


Figure 2.1: Schematic vacuum structure of zero-temperature theory

2.2 Dynamical Supersymmetry Restoration

When the meson expectation values are large enough, non-perturbative effects are turned on and supersymmetric vacua are realized in this sector. It is easily seen from the IR. High meson vevs turn the dual quarks and antiquarks very massive and they are integrated out in the low energy effective theory. The remaining fields fields constitute a super-Yang-Mills theory with N_f^2 single chiral superfields (mesons) and it has N supersymmetric vacua.

The superpotential resumes to

$$W = Nh^\nu \Lambda_m^{3-\nu} \det(\Phi)^{1/N} - h\mu^2 \text{Tr}\Phi \quad (2.5)$$

We can use the gauge symmetry to diagonalize Φ . It is possible to solve the F-term equations determining that the VEVs of Φ eigenvalues, ϕ_i , are all equal to ϕ_S where

$$(h\phi_S)^{\nu-1} = \mu^2 \Lambda_m^{\nu-3} \quad \text{and} \quad \langle \Phi \rangle = \phi_S \mathbb{I}_{N_f} \quad (2.6)$$

Such vacuum is therefore supersymmetric and this mechanism is commonly known as dynamical Supersymmetry restoration[4].

Note that

$$\text{for } \mu \ll \Lambda_m, \quad \text{we have } \mu \ll \phi \ll \Lambda_m \quad (2.7)$$

which enforces the longevity of the metastable vacuum as we will see in the next section. The relation above also keeps the field vevs below the Landau pole, validating the magnetic phase description.

2.3 Metastable vacuum decay

The tunneling rate will largely depend on the distance between the metastable and the supersymmetric vacuum. The height of the potential barrier is less significant in cases where the barrier is extremely thick. As we will see, the potential barrier in the ISS model is not tall, but it is definitely thick with the assumption made in (2.7) and the false vacuum decay is strongly suppressed.

The only method we know to analytically calculate the tunneling decay of the false vacuum is through semiclassical approximation [10]. In our case

gravitational effects can be ignored. The relevant factor in the decay rate is

$$\Gamma/V \approx \exp(-S) \quad (2.8)$$

where Γ/V is the decay rate per unit of time per unit of volume and S is the bounce action [10]. The bounce action is calculated using the path in the field configuration space with lowest potential barrier or resistance between false and true vacuum.

In [20], Intriligator, Seiberg and Shih presented a path with a hump barrier taking the dual quarks expectation values Q and \tilde{Q} straight to zero and then turning on the mesons expectation values $\langle \Phi \rangle \sim \phi \times \mathbb{I}_{N_f}$. But a more careful analysis of the scalar potential lead us to consider the possibility of another path having less resistance, a smaller bounce action. This path has no barrier in the classical potential, but it is a longer path in the field configuration space, what cancel its advantage. The path presented in [20] has a bounce action of the order

$$S_{ISS} \approx \frac{\phi_S^4}{\Delta V} = \left[\frac{\Lambda_m}{\mu} \right]^{4(\nu-3)/(\nu-1)} h^{-6} \quad (2.9)$$

where ΔV is the potential height of the nonsupersymmetric vacuum.

We search for the alternative bounce path looking at the pseudomoduli that contains the nonsupersymmetric vacuum. There, the meson and dual quark fields are parametrized according to (2.3), while at the supersymmetric vacuum, the meson fields assume vevs proportional to the identity matrix \mathbb{I}_{N_f} and q and \tilde{q} get zero vev. Therefore, it is convenient to analyze only the paths

where the meson and dual quark fields are of the form

$$\langle \Phi \rangle = \begin{pmatrix} \phi_1 \mathbb{I}_N & 0 \\ 0 & \phi_2 \mathbb{I}_{N_f - N} \end{pmatrix}, \quad \langle q \rangle = \langle \tilde{q}^T \rangle = \begin{pmatrix} Q \mathbb{I}_{N \times N} \\ 0 \end{pmatrix}, \quad (2.10)$$

where we take ϕ_1 and ϕ_2 real for simplification.

Including the nonperturbative term, the scalar potential is given by:

$$\frac{V}{h^2} = 2N |Q\phi_1|^2 + N \left| Q^2 - \mu^2 + \frac{h^{\nu-1}}{\Lambda_m^{\nu-3}} \phi_2^{\nu-1} \right|^2 + (N_f - N) \left| \frac{h^{\nu-1}}{\Lambda_m^{\nu-3}} \phi_1 \phi_2^{\nu-2} - \mu^2 \right|^2 \quad (2.11)$$

Minimizing the potential, we set

$$Q^2 = \mu^2 - (h^{\nu-1}/\Lambda_m^{\nu-3}) \phi_2^{\nu-1} \quad (2.12)$$

and we get

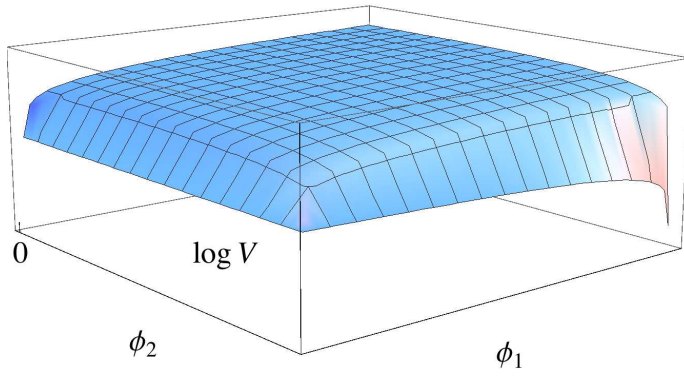
$$\frac{V}{h^2} = 2N |\phi_1|^2 \left| \mu^2 - (h^{\nu-1}/\Lambda_m^{\nu-3}) \phi_2^{\nu-1} \right|^2 + (N_f - N) \left| \frac{h^{\nu-1}}{\Lambda_m^{\nu-3}} \phi_1 \phi_2^{\nu-2} - \mu^2 \right|^2 \quad (2.13)$$

We can see that for ϕ_2 near 0, the potential is minimized at $\phi_1 = 0$. The minimum of the potential is at $V = (N_f - N)h^2\mu^4$ from values of $\phi_2 = 0$ (metastable vacuum) all the way to values below the supersymmetric value ϕ_S (2.6). Thus, classically, the insertion of the nonperturbative term does not create a hump, but a valley around one direction preserving a moduli space that will be lifted by perturbative effects, since this moduli is not supersymmetric, as it is shown in [20]

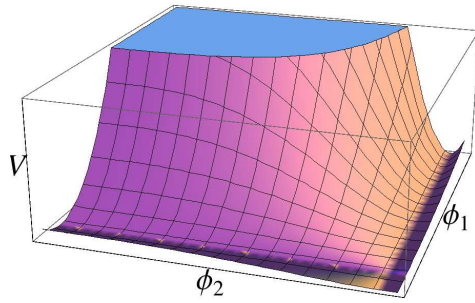
As ϕ_2 gets close to $\phi_S = [\mu^2 \Lambda_m^{\nu-3}]^{1/(\nu-1)} h^{-1}$, the first term in (2.13) is suppressed and the potential is minimized by minimizing the second term which brings ϕ_1 also close to ϕ_S value.

We show below in figure 2.2 the classical potential and the path with no barriers from the metastable vacuum to the supersymmetric vacuum in the field space. Figure 2.2(a) shows the existence of a flat (pseudo)moduli at $\phi_1 = 0$ and a supersymmetric vacuum at $\phi_1 = \phi_2 = \phi_S$. Figure 2.2(b) shows the formation of a valley around the path from the nonsupersymmetric moduli ($\phi_1 = 0$) up to the supersymmetric vacuum. In both pictures, we constrain Q^2 at the values of (2.12).

Once we have the path in the field space of the bounce action we can calculate S . There are a few potentials where a analytical solution exists for the equation of motion of the bounce action. Luckily, our potential fits in the triangle approximation [15], after some consideration. Our bounce action path is a one dimensional path. Hence we can parametrize it by one single parameter z , such that for the first part of the path where $\phi_1 = 0$, $z = \phi_2$ and for the second part of the path where $\phi_2 = \phi_S$, $z = \phi_S + \phi_1$. The classical potential would look like figure (2.3) along the path of minimum barrier (bounce path). The flat part of the potential does not look like a triangle and such flatness leads to infinities in the calculation using the triangle approximation. In the semiclassical approximation, the one loop effects do not change the bounce action and they are taken in account only in the pre-factor of the decay rate [10]. In our case we need to add a small deformation in the classical potential since a flat potential has a disastrous effect on the lifetime of a metastable vacuum, when at one loop level the potential is not flat at all. Our result, within the triangle approximation, will not depend on this deformation.



(a) $\phi_1 = 0$ pseudomoduli and SUSY vacuum



(b) Path to supersymmetric vacuum in $\phi_2 \times \phi_1$ field space

Figure 2.2: Classical potential from Metastable vacuum to SUSY vacuum

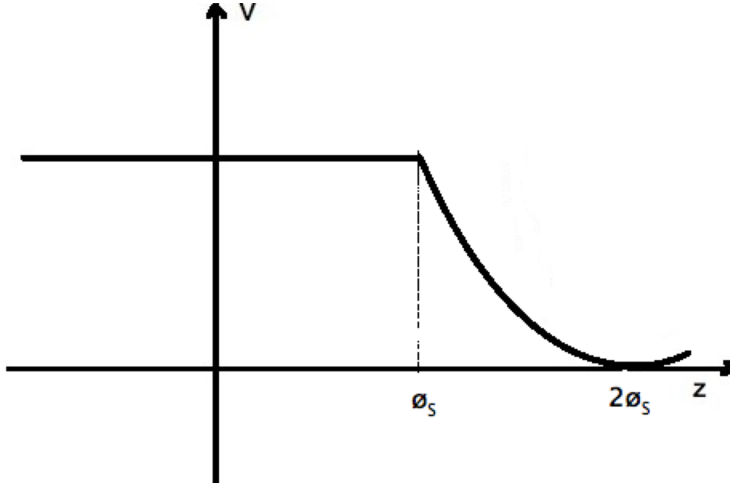


Figure 2.3: Classical potential in bounce path

Therefore, we do not need to make assumptions on the deformation being small or large, but for the sake of a valid semiclassical approximations, quantum effects need to be small. Such approximation will give a lower bound to the half-life of the metastable vacuum, since higher quantum corrections would lift higher the potential barrier, increasing the longevity of the false vacuum.

Given the deformed potential along the bounce path, figure (2.5), the bounce action is calculated by integrating the euclidian action along the bounce solution and subtracting the euclidian action calculated along a false vacuum configuration. Following the prescription found in [15], our bounce solution is a nucleated bubble with boundary conditions that fall in the second case described in [15] in the triangle approximation. Calculating the bounce action, we find the same approximate result as in equation (2.9):

$$S \approx \frac{\phi_S^4}{\Delta V} = \left[\frac{\Lambda_m}{\mu} \right]^{4(\nu-3)/(\nu-1)} h^{-6} \quad (2.14)$$

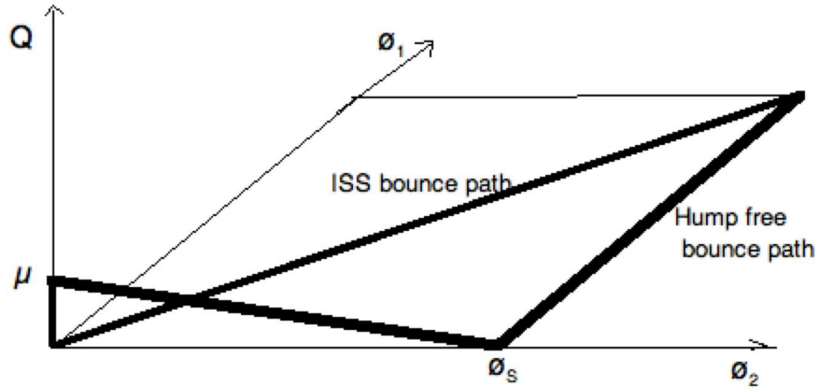


Figure 2.4: ISS and hump free bounce paths in 3D field space

Therefore, both bounce actions are parametrically large and the metastable vacuum decay rate is strongly suppressed turning it into a cosmologically stable vacuum. If we find ourselves in such metastable vacuum we wouldn't be able to distinguish it from a true vacuum!

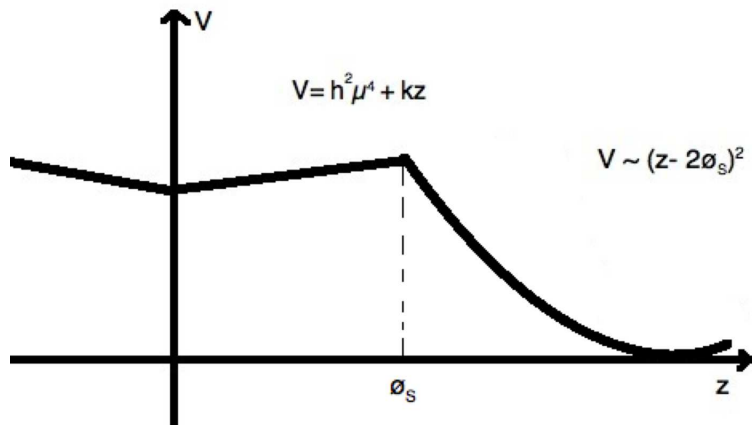


Figure 2.5: Potential along the bounce path with moduli lifted

Chapter 3

Cosmological History of Metastable Supersymmetry Breaking

In the former chapter we saw that the metastable vacuum can have parametrically long lifetime, being protected from tunneling. Hence, they are phenomenologically viable candidates for Supersymmetry breaking.

In this chapter, we will be interested in this question from a cosmological perspective. We will follow closely [17]. Other works tried to answer this same question with similar results [1, 12].

Just the fact that there exists a meta-stable vacuum in the zero temperature field theory is not enough to guarantee that we will end up in it (and not in the susy-vacuum), as the Universe cools from high-temperatures. One way to get a better understanding of this issue is to look at the phase structure of the free energy at different temperatures. We can get some idea about the situation by looking at the equilibrium thermal properties of this theory at finite temperature [11, 14, 23, 29]. We calculate the free energy as a function of the quark and the meson fields. At high enough temperature, we expect that free energy has a trough at the origin of field space, because the fields are massless there and the entropy is therefore higher. We calculate the mass-

matrices for the fields in the quark and meson directions to get an idea about the free-energy in those directions. Indeed, when we do this, we end up finding that as the temperature is lowered, the second order phase transition in the quark direction happens first. There is no (second order) phase transition in the meson direction, all the way down to $T \sim 0$. From these, we conclude that as the temperature drops, the Universe winds up in a susy-breaking phase.

This argument implies that the meta-stable vacuum is plausible, but we should add that this in itself is not completely conclusive.

The reason we use the free energy to calculate the evolution of the expectation values of the fields is that we assume the particles are in a thermal bath and the Universe cools down adiabatically. In this case the minimum of the free energy is the point of minimum non-entropic energy in a system in thermal equilibrium at a given temperature. The free energy is a purely equilibrium quantity and the dynamics of the fields as they interact with a thermal bath could be more complicated. To fully understand the situation, we need to do a calculation that incorporates finite temperature effects *and* dynamics. We need to use the evolution of the field at finite temperature: we could use the imaginary-time formulation and calculate the friction-type term for the field-equation in the thermal bath. We do not report on this calculation here, but the punch-line of the preliminary calculation is that at least for some initial values of the fields, we do evolve and end up in the susy-breaking vacuum. The free energy equations give us an idea about this phase structure, as is clear from the pictures below. In each picture two separate

situations are plotted together: one in the scalar mesons direction with zero squark vev and another in the squark direction with zero scalar meson vev. In 3.1(a), at high temperature the free energy drives the scalar expectation values to zero. In 3.1(b), the plot is at lower temperatures close to a threshold where the free energy in the squark direction develops a minimum away from zero, while in the meson direction it develops a potential barrier. Finally in 3.1(c), at zero temperature, the meta-stable vacuum in the squark direction remains cosmologically stable [20] due to the large (thick but not high) potential barrier in the scalar meson direction, where the susy vacuum is located.

One important assumption is that the Seiberg transition is a post-inflation phenomenon. The reheating temperature is higher than the scale ϕ_S of the supersymmetric vacuum. With this assumption, there will be no relevant minimum besides the origin in field space.

The unsolved problem of initial value of the scalar mesons after the Seiberg transition allow other possibilities that are not considered in the present work. If initially, the scalar mesons are located far away in field space, they will execute large amplitude oscillations. Then, if both the Hubble friction and the interactions of the meson fields with the heat bath are small enough, these oscillations might bring the meson fields in the vicinity of the susy vacuum and possibly they stay there, once the trough at the origin is too far away.

These assumptions are made when the scalar fields are not in equilibrium with the rest of the universe and therefore we should not rely on an equilibrium calculation of the free energy to describe this system in these con-

ditions. It is then plausible, that as the universe cools, the meson fields find themselves trapped in the susy state. However in an adiabatic evolution of the universe it is appropriate to use thermodynamics of equilibrium to describe the system. This is what the body of this chapter will make explicit.

In the next section, we present the calculation of the equilibrium free energy of this theory along the quark and meson directions by calculating the mass matrices for the appropriate fields and expressing the free energy in the high-temperature limit. The interpretation of this object as the temperature is lowered is the subject of section 3.2.

3.1 Free Energy

Our aim now, is to look at the ISS model, and calculate the finite temperature effective potential (free energy) up to one loop. We want to see how the effective potential changes when we turn on temperature. This will give us a clue about the possible phase transitions that could happen, as the universe cooled. The standard procedure for calculating the finite-temperature effective potential is to shift the relevant background fields (in our case the scalar quarks and mesons) and use the resulting quadratic pieces in the action to do the computation. So essentially, we need to know what the masses of the various fields are, as a result of the shifts in the backgrounds. It is the calculation of these mass matrices, that we undertake next. For the sake of simplicity, we will take the parameters h and μ as well as the shifts in the background fields to be real numbers.

3.1.1 Mass Matrices in the Meson Directions

We first calculate the masses of the various fields when a background field is turned on in the meson direction, with the scalar quarks set to zero. In the next subsection we will turn on the squarks and turn off the mesons. Once we know the mass matrices in both these directions, we can draw some conclusions about the free energy and the phase structure as a function of temperature.

Decomposing the meson chiral superfield into a background, trace and a traceless part,

$$\Phi = \left(\varphi + \frac{\Phi_0}{\sqrt{N_f}} \right) \mathbb{I} + \hat{\Phi}, \quad (3.1)$$

we can expand the nonperturbative term in the superpotential:

$$\begin{aligned} AN(\det \Phi)^{1/N} &= AN\varphi^\nu \exp \left(\frac{1}{N} \text{Tr} \ln \left(\mathbb{I} + \frac{\Phi_0}{\sqrt{N_f}\varphi} \mathbb{I} + \frac{\hat{\Phi}}{\varphi} \right) \right) \sim \\ &AN\varphi^\nu \exp \left(\frac{1}{N} \left(\frac{\Phi_0 \sqrt{N_f}}{\varphi} - \frac{\Phi_0^2}{2\varphi^2} - \frac{\text{Tr}(\hat{\Phi}^2)}{2\varphi^2} + \frac{\Phi_0^3}{3\sqrt{N_f}\varphi^3} \right) \right) \sim \\ &A\varphi^\nu \left(N + \frac{\Phi_0 \sqrt{N_f}}{\varphi} + \frac{(\nu-1)\Phi_0^2}{2\varphi^2} - \frac{\text{Tr}(\hat{\Phi}^2)}{2\varphi^2} + \frac{\Phi_0^3(\nu-1)(\nu-2)}{6\sqrt{N_f}\varphi^3} - \frac{(\nu-2)\Phi_0 \text{Tr}(\hat{\Phi}^2)}{2\sqrt{N_f}\varphi^3} \right) \end{aligned}$$

where we named $A = h^\nu \Lambda_m^{3-\nu}$.

From this, we can read off the terms that contribute to the fermion masses in the Lagrangian:

$$\mathcal{L} \supset h\varphi \text{Tr}(\psi_q \psi_{\bar{q}}) + \frac{A\varphi^{\nu-2}(\nu-1)}{2} \psi_{\phi_0} \psi_{\phi_0} - \frac{A\varphi^{\nu-2}}{2} \text{Tr}(\psi_{\hat{\phi}} \psi_{\hat{\phi}}) + h.c. \quad (3.2)$$

showing that there are $N \times N_f$ Dirac fermions with mass $h\varphi$; 1 Majorana fermion with mass $A\varphi^{\nu-2}(\nu-1)$ and $(N_f^2 - 1)$ Majorana fermions with mass $A\varphi^{\nu-2}$.

| # of weyl fermions | fermion fields | mass |
|--------------------|----------------------------|---------------------------|
| $2N \times N_f$ | $\psi_q, \psi_{\tilde{q}}$ | $h\varphi$ |
| 1 | ψ_{ϕ_0} | $A\varphi^{\nu-2}(\nu-1)$ |
| $(N_f^2 - 1)$ | $\psi_{\hat{\phi}}$ | $A\varphi^{\nu-2}$ |

Table 3.1: fermions masses, meson direction

To calculate the scalar masses from the scalar potential, we first compute the F-terms.

$$F_{\phi_0} = \frac{h}{\sqrt{N_f}} \text{Tr}(q\tilde{q}) - h\mu^2 \sqrt{N_f} + \quad (3.3)$$

$$+ A\varphi^\nu \left(\frac{\sqrt{N_f}}{\varphi} + \frac{\nu-1}{\varphi^2} \phi_0 + \frac{(\nu-1)(\nu-2)}{2\varphi^3 \sqrt{N_f}} \phi_0^2 \right) \quad (3.4)$$

$$F_{\hat{\phi}} = h\tilde{q}q + A\varphi^\nu \left(-\frac{\hat{\phi}^t}{\varphi^2} - \frac{(\nu-2)}{\sqrt{N_f}\varphi^3} \phi_0 \hat{\phi}^t \right) \quad (3.5)$$

$$F_q = h(\phi\tilde{q})^t \supset h(\varphi\tilde{q})^t \quad (3.6)$$

$$F_{\tilde{q}} = h(\phi q)^t \supset h(\varphi q)^t \quad (3.7)$$

Consequently, the scalar potential will have the following quadratic terms:

$$V_{\text{scalar}} \supset (A\varphi^{\nu-1} - h\mu^2) \left[\text{Tr}(q\tilde{q})h + \frac{(\nu-1)(\nu-2)A\varphi^{\nu-3}}{2} \phi_0^2 \right] + c.c. + \quad (3.8)$$

$$|A|^2 \varphi^{2\nu-4} ((\nu-1)^2 |\phi_0|^2 + |\hat{\phi}|^2) + h^2 \varphi^2 (|\tilde{q}|^2 + |q|^2) \quad (3.9)$$

where the scalar masses are extracted and shown in table 3.2.

3.1.2 Mass Matrices in the Quark Directions

The mass matrices in the quark directions are more complicated than in the meson directions because there are contributions from the D-terms.

| # of real scalars | scalar fields | $mass^2$ |
|-------------------|--------------------------------|--|
| $2(N_f^2 - 1)$ | $\widehat{\phi}$ | $ A ^2 \varphi^{2\nu-4}$ |
| 1 | $Im \phi_0$ | $ A ^2 \varphi^{2\nu-4} (\nu - 1)^2 -$ $- Re [(A\varphi^{\nu-1} - h\mu^2)^* (\nu - 1)(\nu - 2) A\varphi^{\nu-3}]$ |
| 1 | $Re \phi_0$ | $ A ^2 \varphi^{2\nu-4} (\nu - 1)^2 +$ $+ Re [(A\varphi^{\nu-1} - h\mu^2)^* (\nu - 1)(\nu - 2) A\varphi^{\nu-3}]$ |
| $N \times N_f$ | $Re(q + \tilde{q}^t)/\sqrt{2}$ | $h^2 \varphi^2 + Re(A\varphi^{\nu-1} - h\mu^2)h$ |
| $N \times N_f$ | $Im(q + \tilde{q}^t)/\sqrt{2}$ | $h^2 \varphi^2$ |
| $N \times N_f$ | $Re(q - \tilde{q}^t)/\sqrt{2}$ | $h^2 \varphi^2 - Re(A\varphi^{\nu-1} - h\mu^2)h$ |
| $N \times N_f$ | $Im(q - \tilde{q}^t)/\sqrt{2}$ | $h^2 \varphi^2$ |

Table 3.2: real scalar squared masses, meson direction

We start by classifying the various sectors according to their transformation properties under the global symmetries. We take the shifts in the form: $\langle \tilde{q}_1 \rangle = \langle q_1 \rangle = Q \mathbb{I}$, Q real. The column vectors are $N \times N_e$ where $N_e = N_f - N$. The subscript stands for electric. N_e is the same as N_c , the number of colors in the original (microscopic) theory, namely SQCD, but we prefer to think of it purely in terms of the dual theory.

There are four sectors that do not mix with each other in the Lagrangian. We will use this fact to our advantage in calculating the mass matrices. These sectors are:

1. $N_e \times N_e : \phi_{22},$
2. $N_e \times N : \tilde{q}_2, \phi_{21},$
3. $N \times N_e : q_2, \phi_{12},$
4. $N \times N : q_1, \tilde{q}_1, \phi_{11}, V.$

The V in the last line is the vector superfield, it gets massive through a Higgs mechanism.

Now we look at the masses of the various fields sector by sector. To start off, in the $N_e \times N_e$ sector, there are $N_e^2 \times (\text{complex scalars} + \text{Weyl Fermions})$, and all of them remain entirely massless (at tree level). But it is in this sector that supersymmetry is broken by a positive contribution in the scalar potential. Decomposing Φ_{22} into trace and traceless parts, we get

$$\Phi_{22} = \frac{\Phi_{22}^0}{\sqrt{N_e}} \mathbb{1} + \widehat{\Phi}_{22}; \quad F_{\Phi_{22}^0} \supset -h\mu\sqrt{N_e}.$$

Hence

$$V_{\text{scalar}} \geq N_e h^2 \mu^4.$$

It is easiest to deal with the two mixed electric/magnetic sectors (2 and 3) together. Together, there are $2N_e N \times (2 \text{ complex scalars} + 1 \text{ Dirac fermion})$. The fermionic masses arise from terms like

$$hQ \text{Tr}(\Psi_{12}^\phi \Psi_2^q) + hQ \text{Tr}(\Psi_2^{\tilde{q}} \Psi_{21}^\phi) + h.c., \quad (3.10)$$

and these give rise to a Dirac mass of hQ . To calculate the bosonic masses, we need the scalar potential in the quark direction which can be calculated easily enough from the superpotential and the F-terms. The F-terms $F_{q_1}, F_{\tilde{q}_1}$ do not give rise to scalar masses in sectors 2 and 3 because the scalars from these sectors have zero vevs. The relevant non-vanishing ones are

$$F_{\phi_{12}} = h(\tilde{q}_2 q_1)^t \supset hQ(\tilde{q}_2)^t \quad (3.11)$$

| # of real scalars | scalar fields | $mass^2$ |
|-------------------|------------------------------------|--------------------|
| $4N \times N_e$ | ϕ_{12} and ϕ_{21} | $h^2 Q^2$ |
| $N \times N_e$ | $Re(q_2 + \tilde{q}_2^t)/\sqrt{2}$ | $h^2(Q^2 + \mu^2)$ |
| $N \times N_e$ | $Re(q_2 - \tilde{q}_2^t)/\sqrt{2}$ | $h^2(Q^2 - \mu^2)$ |
| $N \times N_e$ | $Im(q_2 + \tilde{q}_2^t)/\sqrt{2}$ | $h^2 Q^2$ |
| $N \times N_e$ | $Im(q_2 - \tilde{q}_2^t)/\sqrt{2}$ | $h^2 Q^2$ |

Table 3.3: real scalar squared masses, sectors 2 and 3

$$F_{\phi_{21}} = h(\tilde{q}_1 q_2)^t \supset hQ(q_2)^t \quad (3.12)$$

$$F_{\phi_{22}} = h(\tilde{q}_2 q_2)^t - h\mu^2 \times \mathbb{I} \quad (3.13)$$

$$F_{\tilde{q}_2} = h(q_1 \phi_{12} + q_2 \phi_{22}) \supset hQ\phi_{12} \quad (3.14)$$

$$F_{q_2} = h(\phi_{21} \tilde{q}_1 + \phi_{22} \tilde{q}_2) \supset hQ\phi_{21} \quad (3.15)$$

Therefore, the scalar potential contains the quadratic terms:

$$V_{scalar} \supset h^2 (Q^2 |\tilde{q}_2|^2 + Q^2 |q_2|^2 - \mu^2 \text{Tr}(\tilde{q}_2 q_2 + h.c.) + Q^2 |\phi_{12}|^2 + Q^2 |\phi_{21}|^2) \quad (3.16)$$

where in our notation modulus squared of matrices means trace over the product of the matrix and its adjoint. As we see, $2N \times N_e$ complex scalars (ϕ_{12} and ϕ_{21}) get squared mass $h^2 Q^2$, $2N \times N_e$ real scalars ($Re(q_2 \pm \tilde{q}_2^t)/\sqrt{2}$) split their masses into $h^2(Q^2 \pm \mu^2)$ and another $2N \times N_e$ real scalars ($Im(q_2 \pm \tilde{q}_2^t)/\sqrt{2}$) get mass $h^2 Q^2$. See table (3.3).

Now we turn to sector 4. First, we separate out the background:

$$q_1 = Q\mathbb{I} + \hat{q}_1 ; \quad \tilde{q}_1 = Q\mathbb{I} + \hat{\tilde{q}}_1 \quad (3.17)$$

Some of the fermion masses arise from the terms

$$g\sqrt{2}Q \operatorname{Tr}(\lambda\Psi_1^q) - g\sqrt{2}Q \operatorname{Tr}(\lambda\Psi_1^{\tilde{q}}) + h.c. \quad (3.18)$$

where gauginos λ^a , and the traceless $(\Psi_1^q - \Psi_1^{\tilde{q}})/\sqrt{2}$ have equal masses $2gQ$.

From the Kähler potential, the vector bosons A_μ get a mass $2gQ$. The traceless part of $Im\left((\hat{q}_1 - \hat{\tilde{q}}_1)/\sqrt{2}\right)$ is gauged away and the traceless part of the scalars $Re\left((\hat{q}_1 - \hat{\tilde{q}}_1)/\sqrt{2}\right)$ get their masses from the F-terms (to be calculated) and from the D-terms. The contribution to this squared mass from the D-terms can be read off from

$$\begin{aligned} \frac{g^2}{2} \sum_a (\operatorname{Tr}(q_1^\dagger t^a q_1 - \tilde{q}_1^\dagger t^a \tilde{q}_1))^2 &\supset \frac{g^2}{2} \sum_a (Q \operatorname{Tr}(t^a (\hat{q}_1 - \hat{\tilde{q}}_1 + \hat{q}_1^\dagger - \hat{\tilde{q}}_1^\dagger)))^2 = \\ \frac{g^2}{2} \sum_a (Q \operatorname{Tr}(2 \operatorname{Re}[t^a (\hat{q}_1 - \hat{\tilde{q}}_1)]))^2 &= 4g^2 Q^2 \sum_a \left(\operatorname{Tr}(\operatorname{Re}[t^a (\hat{q}_1 - \hat{\tilde{q}}_1)/\sqrt{2}]) \right)^2 \end{aligned} \quad (3.19)$$

to be $4g^2 Q^2$. The scalar $Im(\operatorname{Tr}(q_1 - \tilde{q}_1))/\sqrt{2}$ and the fermion $\operatorname{Tr}(\Psi_1^q - \Psi_1^{\tilde{q}})/\sqrt{2}$ remain massless at tree level. But $Re(\operatorname{Tr}(q_1 - \tilde{q}_1))/\sqrt{2}$ receives a contribution from the F-terms.

The shifts in q_1 and \tilde{q}_1 give rise to terms of the form

$$hQ\Psi_{11}^\phi(\Psi_1^q + \Psi_1^{\tilde{q}}) + h.c.$$

From these, the $2N^2$ Weyl fermions (Ψ_{11}^ϕ) and $(\Psi_1^q + \Psi_1^{\tilde{q}})/\sqrt{2}$ acquire a mass of $hQ\sqrt{2}$ each. Their respective scalar superpartners acquire mass through the scalar potential. Writing the relevant terms in the F-terms, using (3.17), we have

$$F_{\phi_{11}} = h \left((Q^2 - \mu^2) \mathbb{I} + Q\sqrt{2} \frac{\hat{q}_1 + \hat{\tilde{q}}_1}{\sqrt{2}} + \hat{q}_1 \hat{q}_1 \right)$$

| # fields | fields | mass |
|-----------|--|--------------|
| $N^2 - 1$ | $A^{\mu,a}$ | $2gQ$ |
| $N^2 - 1$ | λ^a | $2gQ$ |
| $N^2 - 1$ | traceless $(\Psi_1^q - \bar{\Psi}_1^q)/\sqrt{2}$ | $2gQ$ |
| $2N^2$ | Ψ_{11}^ϕ | $hQ\sqrt{2}$ |
| $2N^2$ | $(\Psi_1^q + \bar{\Psi}_1^q)/\sqrt{2}$ | $hQ\sqrt{2}$ |

Table 3.4: vector boson and fermion masses, sector 4

and $F_{q_1} \supset hQ\phi_{11}$, $F_{\tilde{q}_1} \supset hQ\phi_{11}$. Hence, the quadratic terms in the scalar potential are,

$$V_{scalar} \supset h^2 \left(2Q^2 |\phi_{11}|^2 + 2Q^2 \left| \frac{\hat{q}_1 + \hat{\bar{q}}_1}{\sqrt{2}} \right|^2 + (Q^2 - \mu^2) \left(\text{Tr}(\hat{q}_1 \hat{\bar{q}}_1) + c.c \right) \right) \quad (3.20)$$

This shows that among the real scalars, $2N^2$ get squared masses $2h^2Q^2$, N^2 get squared masses $h^2(3Q^2 - \mu^2)$, and N^2 get squared masses $2h^2Q^2$. The corresponding fields are ϕ_{11} , $Re(\hat{q}_1 + \hat{\bar{q}}_1)/\sqrt{2}$ and $Im(q_1 + \tilde{q}_1)/\sqrt{2}$ respectively. The terms $Re(\hat{q}_1 - \hat{\bar{q}}_1)/\sqrt{2}$ get mass from above and from the D-terms, splitting the field matrix into a trace part with mass $h^2(\mu^2 - Q^2)$ and $N^2 - 1$ traceless components with mass $h^2(\mu^2 - Q^2) + 4g^2Q^2$.

The vector boson, gaugino and fermion masses are presented in table (3.4), and the scalar masses are in table (3.5).

3.1.3 Effective potential

The effective potential at finite temperature is the free energy of a system in a thermal bath. In thermal equilibrium, there is no time dependence

| # of real bosons | fields | $mass^2$ |
|------------------|---|------------------------------|
| N^2 | $Re(\widehat{q}_1 + \widehat{\widetilde{q}}_1)/\sqrt{2}$ | $h^2(3Q^2 - \mu^2)$ |
| $2N^2$ | ϕ_{11} | $2h^2Q^2$ |
| N^2 | $Im(\widehat{q}_1 + \widehat{\widetilde{q}}_1)/\sqrt{2}$ | $2h^2Q^2$ |
| $N^2 - 1$ | traceless $Re(\widehat{q}_1 - \widehat{\widetilde{q}}_1)/\sqrt{2}$ | $h^2(\mu^2 - Q^2) + 4g^2Q^2$ |
| 1 | $Tr\left(Re(\widehat{q}_1 - \widehat{\widetilde{q}}_1)/\sqrt{2}\right)$ | $h^2(\mu^2 - Q^2)$ |
| 1 | $Tr\left(Im(\widehat{q}_1 - \widehat{\widetilde{q}}_1)/\sqrt{2}\right)$ | 0 |

Table 3.5: real squared masses for bosons, sector 4

and the different phases correspond to local minima of the free energy.

The finite temperature effective potential up to one loop is given by [14]

$$V(\phi_{cl}) = V_{tree}(\phi_{cl}) + V_1^0(\phi_{cl}) + V_1^T(\phi_{cl})$$

where $V_{tree}(\phi_{cl})$ is the classical piece. The one-loop correction, $V_1^T(\phi_{cl})$, for a generic theory is:

$$\begin{aligned}
V_1^T(\phi_{cl}) \approx & -\frac{\pi^2 T^4}{90} \left(N_B + \frac{7}{8} N_F \right) + \frac{T^2}{24} \left[\sum_i (M_S^2)_i + 3 \sum_i (M_V^2)_i + 2 \sum_i (M_F^2)_i \right] \\
& - \frac{T}{12\pi} \left[\sum_i (M_S^3)_i + 3 \sum_i (M_V^3)_i \right] + \dots
\end{aligned} \tag{3.21}$$

and $V_1^0(\phi_{cl})$ is the zero-temperature piece, $(M_S)_i$, $(M_V)_i$ and $(M_F)_i$ are mass-matrix eigenvalues for the real scalars, vector bosons and Weyl fermions respectively, and $N_B = N_F$ is the number of bosonic/fermionic degrees of freedom, paired by supersymmetry. What we have done here is to follow the standard practice and split off the one-loop, finite-temperature effective potential into a part that is independent of temperature (and therefore is the same as the

zero-temperature effective potential) and then do a high-temperature ($T \gg$ masses) expansion on the remaining (temperature-dependant) piece. The zero temperature piece is calculated using the usual supersymmetric generalization of the Coleman-Weinberg formula [11]:

$$V_1^0 = \frac{1}{64\pi^2} \text{STr } \mathcal{M}^4 \log \frac{\mathcal{M}^2}{\Lambda^2}, \quad (3.22)$$

where \mathcal{M} stands for the full mass-matrix, with the supertrace providing the negative sign for the fermionic terms and counting the degrees of freedom of real scalars, vector bosons and fermions as in (1.1).

Armed with the above expressions and the mass-matrices from the last section, its easy to calculate the finite-temperature effective potential. In the following, we only keep the terms that are quartic and quadratic in temperature. In the case of background fields in the meson direction, we find:

$$V_{tree}(\varphi) = N_f |(A\varphi^{\nu-1} - h\mu^2)|^2, \quad (3.23)$$

$$\begin{aligned} V_1^0(\varphi) = & \frac{1}{64\pi^2} \left(-2|A|^4 \varphi^{4\nu-8} (\nu-1)^4 \log \frac{|A|^2 \varphi^{2\nu-4} (\nu-1)^2}{\Lambda^2} + \right. \\ & + [|A|^2 \varphi^{2\nu-4} (\nu-1)^2 - \text{Re} [(A\varphi^{\nu-1} - h\mu^2)^* (\nu-1)(\nu-2) A\varphi^{\nu-3}]]^2 \times \\ & \times \log \frac{|A|^2 \varphi^{2\nu-4} (\nu-1)^2 - \text{Re} [(A\varphi^{\nu-1} - h\mu^2)^* (\nu-1)(\nu-2) A\varphi^{\nu-3}]}{\Lambda^2} + \\ & + [|A|^2 \varphi^{2\nu-4} (\nu-1)^2 + \text{Re} [(A\varphi^{\nu-1} - h\mu^2)^* (\nu-1)(\nu-2) A\varphi^{\nu-3}]]^2 \times \\ & \times \log \frac{|A|^2 \varphi^{2\nu-4} (\nu-1)^2 + \text{Re} [(A\varphi^{\nu-1} - h\mu^2)^* (\nu-1)(\nu-2) A\varphi^{\nu-3}]}{\Lambda^2} + \\ & + NN_f h^2 (h\varphi^2 + \text{Re}(A\varphi^{\nu-1} - h\mu^2))^2 \log \frac{h^2 \varphi^2 + \text{Re}(A\varphi^{\nu-1} - h\mu^2)h}{\Lambda^2} - \\ & \left. - 2NN_f h^4 \varphi^4 \log \frac{h^2 \varphi^2}{\Lambda^2} + NN_f h^2 (h\varphi^2 - \text{Re}(A\varphi^{\nu-1} - h\mu^2))^2 \log \frac{h^2 \varphi^2 - \text{Re}(A\varphi^{\nu-1} - h\mu^2)h}{\Lambda^2} \right), \end{aligned} \quad (3.24)$$

$$\begin{aligned}\bar{V}_1^T(\varphi) = & -\frac{\pi^2 T^4}{24} ((N_f + N)^2 - 1) + \\ & + \frac{T^2}{6} \{ (N_F^2 - 1) |A^2| \varphi^{2\nu-4} + |A^2| \varphi^{2\nu-4} (\nu - 1)^2 + 2NN_F h^2 \varphi^2 \}.\end{aligned}\quad (3.25)$$

Similarly, for the quark direction:

$$V_{tree}(Q) = N_e h^2 \mu^4 + N h^2 (Q^2 - \mu^2)^2, \quad (3.26)$$

$$\begin{aligned}V_1^0(Q) = & \frac{1}{64\pi^2} (-2NN_e h^4 Q^4 \log \frac{h^2 Q^2}{\Lambda^2} + NN_e h^4 (Q^2 + \mu^2)^2 \log \frac{h^2 (Q^2 + \mu^2)}{\Lambda^2} + \\ & + NN_e h^4 (Q^2 - \mu^2)^2 \log \frac{h^2 (Q^2 - \mu^2)}{\Lambda^2} + N^2 h^4 (3Q^2 - \mu^2)^2 \log \frac{h^2 (3Q^2 - \mu^2)}{\Lambda^2} - \\ & - 4N^2 h^4 Q^4 \log \frac{2h^2 Q^2}{\Lambda^2} + (N^2 - 1)(h^2(\mu^2 - Q^2) + 4g^2 Q^2)^2 \log \frac{h^2(\mu^2 - Q^2) + 4g^2 Q^2}{\Lambda^2} + \\ & + (h^2(\mu^2 - Q^2))^2 \log \frac{h^2(\mu^2 - Q^2)}{\Lambda^2} - (N^2 - 1)(4g^2 Q^2)^2 \log \frac{4g^2 Q^2}{\Lambda^2}),\end{aligned}\quad (3.27)$$

$$\bar{V}_1^T(Q) = -\frac{\pi^2 T^4}{24} ((N_f + N)^2 - 1) + \frac{T^2 Q^2}{3} \{ 4(N^2 - 1)g^2 + N(2N_F + N)h^2 \}.\quad (3.28)$$

With these explicit forms for the finite temperature effective potential, we will be able to draw some conclusions about the nature of the phase-transitions in the next section.

Armed with these expressions and the mass-matrices from the previous sub-sections, we can calculate the explicit forms for the free energy.

3.2 Cooling and the Emergence of Different Phases

We want now to understand what happens to the mesons and squarks expectation values φ, Q during the evolution of the universe, as we cool down

from a high temperature. In particular, we want to know the phase structure. As we mentioned in the beginning of the chapter, it is now clear in expressions (3.25) and (3.28) that at large temperatures, $T \gg Q, \varphi$, the minimum of the free energy will be at the origin $Q = \varphi = 0$ and that will be the respective expectation values. As temperatures cool down, zero temperature terms (tree level and 1-loop) start to be relevant in the free energy, shaping their local minima in the free energy. Eventually, as temperature continues to go down, the minimum at the origin will not be the global minimum anymore and the Universe is susceptible to first or second order phase transition. If the phase transition in the squark direction happens at a higher temperature than in the meson direction, then we have at least some reason to believe that we will eventually end up in the susy-breaking phase.

Phase transitions are characterized by a critical temperature T_c . By definition, the critical temperature T_c for a second order phase transition is the temperature at which the second derivative of $V(\varphi, Q, T)$ at the origin, in one of the field directions, changes sign from positive to negative. When this happens, the local minimum (at the origin) in that direction becomes a local maximum and a new minimum forms at some finite field value. As a consequence, the vacuum at the origin becomes unstable, a phase transition takes place, and the fields evolve to the newly formed minimum. Of course, again, we emphasize that we are doing an equilibrium analysis, but we believe that this is enough to give a preliminary, heuristic picture of the field history. A first order phase transition takes place when a global minimum becomes

a local minimum at lower temperatures and thermal activation tunnels to a new global minimum. In the squark direction, the contestant minimum for new global minimum is at $Q = \mu$. In order to find the critical temperatures in the squark direction, we neglect the Coleman-Weinberg correction. Since we are dealing with scales between zero and μ , the Coleman-Weinberg term is small, suppressed by $\frac{h^2}{64\pi^2}$. Looking at the expressions of the tree-level term (3.26) and the one-loop temperature term (3.28), we see that the first order critical temperature T_1^Q is higher than the second order critical temperature T_2^Q , but both will be of the order of μ , the single present energy scale. After temperature reaches the first order critical value, the Universe stays at the phase ($Q = \phi = 0$), now a supercooling state, due to the potential barrier. The decay rate to $Q = \mu$ minimum will be short, since the potential barrier is small and the distance between the two minima in the field space is also small. In parallel, the temperatures continue to go down and it reaches the second order critical temperature, where the Universe definitely phase change to $Q = \mu$ minimum, if it hadn't changed before. Hence the second order critical temperature will be the relevant parameter $T_2^Q = T_c^Q$ to define phase transition to metastable vacuum. Figure (3.2) clarify such aspects, noticing that the free energies at different temperatures have been shifted by constants for comparative reasons.

One last remark. For temperatures $T \sim \mu$ our one-loop temperature correction in the squark direction is not a good approximation, since the masses are of the same order. The exact one-loop temperature contribution can be

found in textbooks [7]. Our result is just a reasonable estimative.

In the calculation of the second order T_c^Q in the quark direction, at $Q = 0$, most particles will be massless and they will increase the entropy and decrease the free energy. At $Q = \mu$, most particles will have mass comparable to the temperature, and they will not contribute as degrees of freedom anymore. Taking this in consideration, we find for the second order critical temperature

$$(T_c^Q)^2 \sim N\mu^2 \quad (3.29)$$

On the other hand, in the meson direction, we see that there is a minimum away from the origin at this temperature scale, but, the local minimum at the origin is still there. At some temperature T_c^φ these two minima will become degenerate ($V(0, T_c^\varphi) = V(\varphi_m, T_c^\varphi)$), but there still is a large potential barrier between them. Tunneling through the barrier can start when the temperature hits T_c^φ , but this phase transition is first order as opposed to the second-order phase transition in the quark direction.

Hence, even if the T_c^φ is of the order of T_c^Q , the Universe will change phase to the metastable vacuum before it can decay to the supersymmetric vacuum.

The calculation of T_c^φ has a few caveats that we will lay on the table. The only two scales involved are μ and ϕ_S and naively we estimate that the temperature would be between this 2 values. In the meson direction, at $\phi = 0$,

most fields are massless and the Coleman-Weinberg term is negligible.

$$V(\phi = 0, T = T_c^\varphi) = N_f h^2 \mu^4 - \frac{(T_c^\varphi)^4 \pi^2}{24} [(N_f + N)^2 - 2N_f N - 1]$$

At $\phi = \phi_S$, the zero temperature part of the free energy is zero (supersymmetric vacuum configuration). The quarks supermultiplets are heavy (masses $\sim h\phi_S$) and integrated out from the free energy. Only the meson supermultiplet is light enough to be counted in the one-loop temperature term, with masses $\ll T_c^\varphi$, giving accuracy of our one loop temperature approximation. Noticing that the quartic term in temperature will dominate,

$$V(\phi = \phi_S, T = T_c^\varphi) \sim -\frac{(T_c^\varphi)^4 \pi^2}{24} N_f^2$$

The critical temperature for the first order phase transition in the mesons direction turns out to be

$$(T_c^\varphi)^2 \sim \frac{2h\mu^2}{\pi N} \sqrt{6N_f} \quad (3.30)$$

Our estimatives show that critical temperature T_c^φ and T_c^Q in equation (3.29), are of the same order, which guarantees that the Universe will change phase to the metastable vacuum, as discussed above.

To confirm our believes, we notice that in the meson direction the origin is always a local minimum for every temperature, even zero temperature and therefore phase transition in the meson direction will always be of first order,

with a very large suppression. In fact, expanding the 1-loop effective potential at zero temperature $V(\varphi, Q, T = 0)$ around the origin we find

$$V(\varphi, Q, T = 0) \sim h^2 \varphi^2, \varphi \sim 0.$$

Finite temperature effects do not change the fact the the origin is still a local minimum in the meson direction. In this case we have

$$V(\varphi, Q, T) \sim T^2 h^2 \varphi^2, \varphi \sim 0.$$

Because the phase transition in the meson directions is first order, it is accomplished through quantum tunneling processes and hence is much more strongly suppressed than the classical phase transition in the quark directions.

To gain a better understanding of the phase transition in the quarks direction we studied the finite temperature effective potential for every value of ϕ and Q close to the critical temperature T_c^Q . The result of this analysis is plotted in Fig. 3.3. From the shape of the effective potential around the origin we immediately realize that the flow of the vev happen in the Q direction and it is not possible for the vev to flow in the ϕ direction.

We are now in the position to form an idea about the phase history as the universe cools down. Let's suppose that we are starting at a temperature $T \gg T_c^Q, T_c^\varphi$. We could for example be in the reheating phase after inflation. At this temperature, the origin of field space is a minimum for the finite temperature effective potential $V(\varphi, Q, T)$, figure 3.1(a). This is qualitatively plausible, since the massless fields make the biggest contribution to entropy.

We also make the assumption that when we start off at this high temperature, the mesons φ and the quarks Q are localized around the origin of field space: $\varphi = 0, Q = 0$ when $T \gg T_c$. As the temperature decreases to $T = T_c^Q$, the curvature of the effective potential $V(\varphi, Q, T)$ at the origin becomes negative in the Q direction but it stays positive in the φ direction:

$$\left(\frac{\partial^2 V}{\partial Q^2} \right)_{\varphi=0, Q=0, T=T_c} < 0,$$

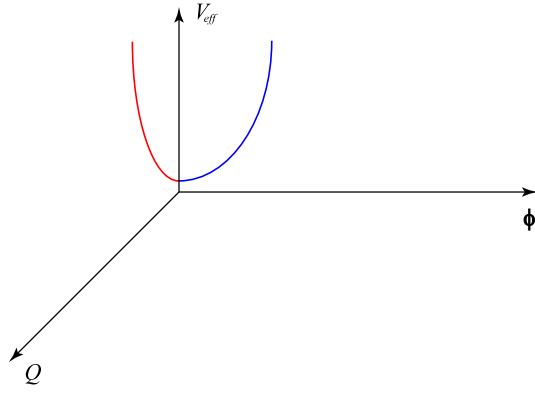
$$\left(\frac{\partial^2 V}{\partial \varphi^2} \right)_{\varphi=0, Q=0, T=T_c} > 0.$$

Also, at $T = T_c^Q$, a new minimum Q_m forms in the Q direction, see figure 3.1(b). As a consequence, a phase transition occurs and the fields move to the newly formed minimum Q_m . As the temperature of the universe continues to decrease, we eventually arrive at $T \sim 0$, see figure 3.1(c), and the minimum Q_m becomes the (meta-stable) non-supersymmetric vacuum $Q_m^0 = \begin{pmatrix} \mu \mathbb{I}_N \\ 0 \end{pmatrix}$. On the meson side, as the temperature drops, the minimum φ_m becomes the supersymmetric vacuum $\varphi_m^0 = \phi_S = \frac{\mu}{h} \frac{1}{\epsilon^{(N_f-3N)/(N_f-N)}}$, but thankfully, phase-transition into the susy phase is suppressed by tunneling at all stages. In writing the expression for the susy-vacuum φ_m^0 , we use the Intriligator et al. convention, with $\epsilon \equiv \mu/\Lambda_m$ where Λ_m is the dynamically generated scale of our (infrared) theory. As mentioned earlier, it is the scale of the Landau pole.

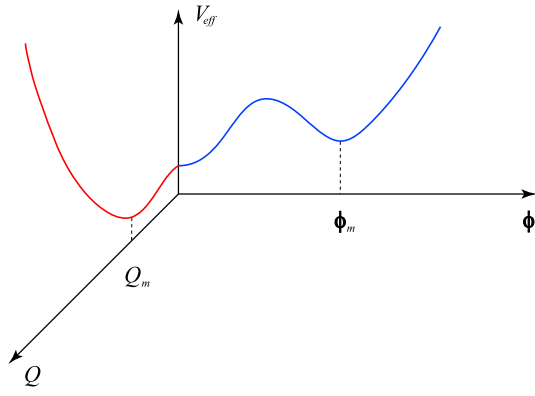
Thus, the phase structure of the theory seems to imply that for reasonably tame initial conditions for the scalar quarks and mesons (namely, they start off near the origin of field space), the phase transitions lead us into the

susy-breaking vacuum at $T \sim 0$:

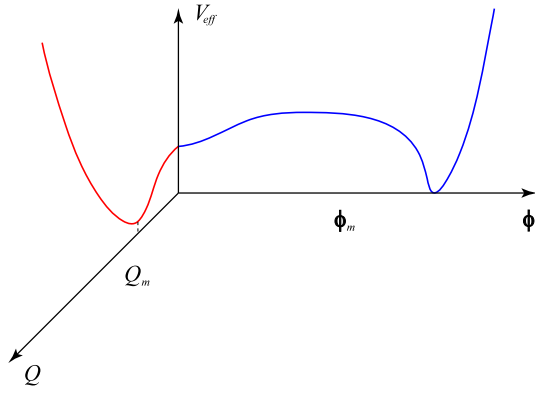
$$\varphi = 0, \quad Q_m^0 = \begin{pmatrix} \mu \mathbb{I}_{N_f} \\ 0 \end{pmatrix}.$$



(a) Effective potential for $T \gg T_c$



(b) Effective potential for $T \sim T_c$



(c) Effective potential for $T = 0$

Figure 3.1: Evolution of the effective potential with temperature

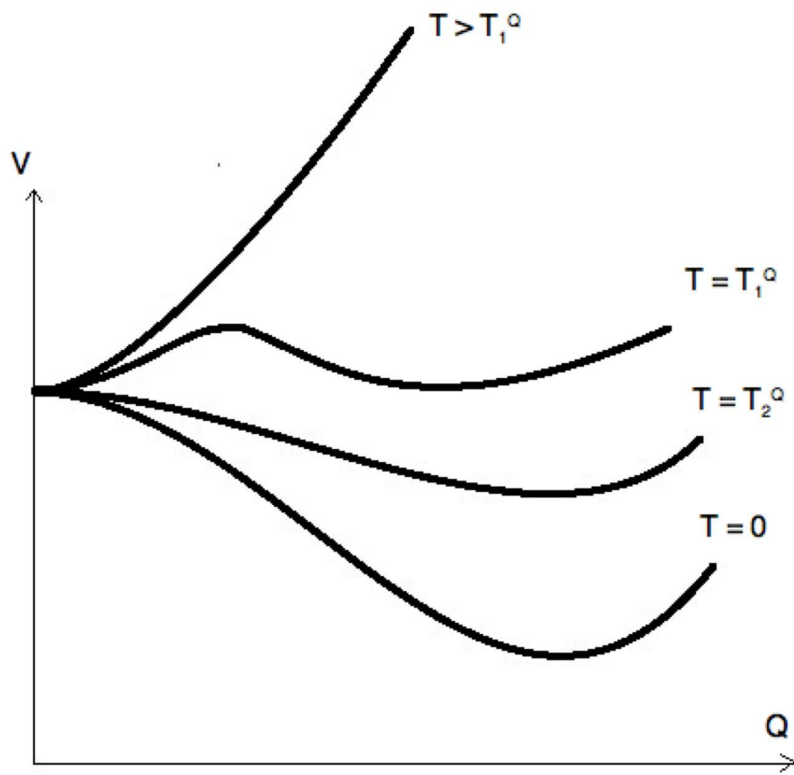


Figure 3.2: Free energy in squark direction at different temperatures. $T_1^Q > T_2^Q = T_c^Q$

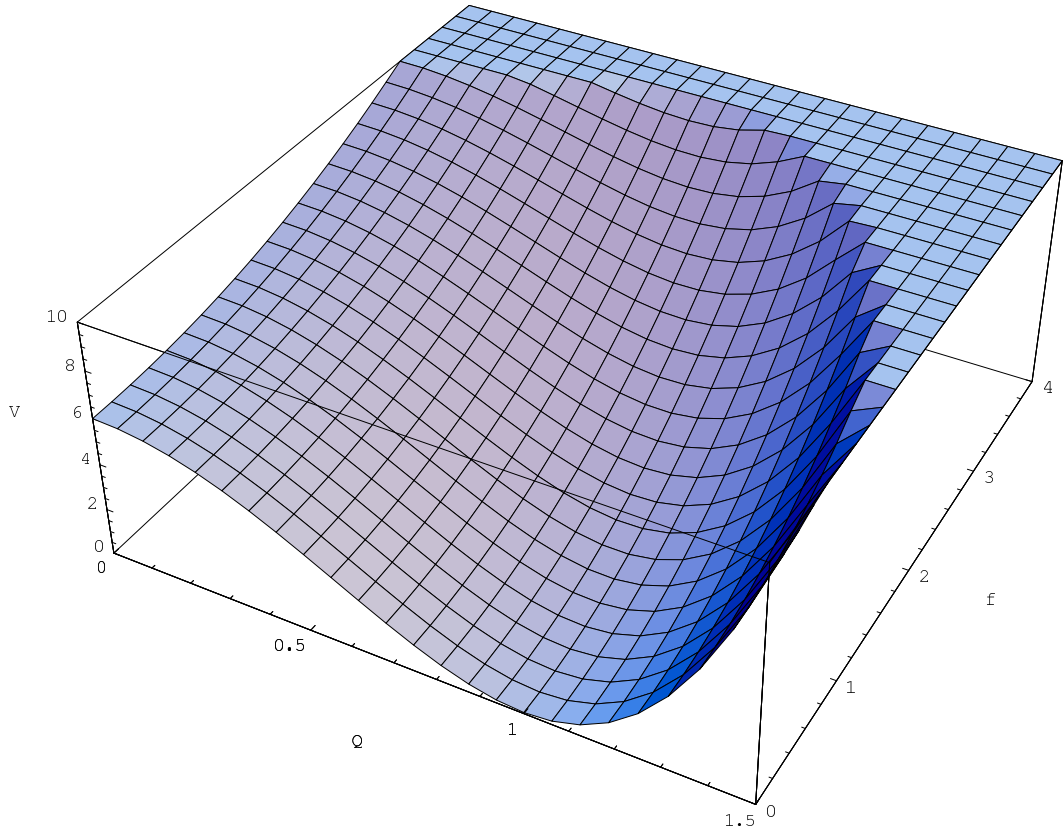


Figure 3.3: Effective potential for every values of ϕ and Q for $T \sim T_c^Q$

Chapter 4

Flavor Gauging

In this chapter we return to zero temperature physics and gauge the flavor symmetry $SU(N_f)$, such that the gauge interaction is weak at the scale μ of the non-supersymmetric vacuum and above, i. e., its Landau pole Λ_f is much smaller than μ . In this frame, the classical moduli space is lifted in a different way and an inverse hierarchy mechanism [30] pushes the masses of the magnetic quarks, q and \tilde{q} , in the nonsupersymmetric vacuum to higher scales close to the supersymmetric vacuum, threatening the longevity of the meta-stable vacuum or even removing the meta-stable vacuum via runaway mechanism. We were able to show in this work that runaway will in most cases not occur and that in most part of the parameter space of the theory the meta-stable vacuum will have a long life. This chapter is based on a ongoing work done by V. Kaplunovsky and I [22].

We will only need to work up to 1-loop calculation to deform the classical moduli space, since it is the dominant contribution. At all energies, the Coleman-Weinberg expression [11] give us the exact 1-loop corrections, but our calculation becomes much simpler at higher energies when we neglect the supersymmetry breaking effects and use supersymmetry nonrenormalization

theorems [19] and RGE equations.

The gauging of the flavor symmetry imposes a new D-term constraint on the classical moduli space and Φ_{22} is found to be diagonal. Under this restriction, we choose to work on the subdomain of the classical moduli space

$$\Phi = \begin{pmatrix} 0 & 0 \\ 0 & \varphi \mathbb{I}_{N_f - N} \end{pmatrix}, \quad q = \begin{pmatrix} \mu \mathbb{I}_N \\ 0 \end{pmatrix}, \quad \tilde{q} = (\mu \mathbb{I}_N \quad 0), \quad (4.1)$$

where we will keep expectation value φ real for simplicity. A $SU(N_f - N)$ gauge symmetry is preserved. Later on section 4.5, we will discourse on the case in which Φ_{22} vev is a general diagonal matrix.

As in chapter 3, we divide the particles according to their Lagrangian interactions in 4 mass matrix sectors. They are:

$$\Phi = \begin{pmatrix} \Phi_{11} & \Phi_{12} \\ \Phi_{21} & \Phi_{22} \end{pmatrix}, \quad q = \begin{pmatrix} q_1 \\ q_2 \end{pmatrix}, \quad \tilde{q} = (\tilde{q}_1 \quad \tilde{q}_2), \quad (4.2)$$

where we call the $(N_f - N) \times (N_f - N)$ Φ_{22} fields by sector 1; the $(N_f - N) \times N$ \tilde{q}_2 and Φ_{21} fields by sector 2; the $N \times (N_f - N)$ q_2 and Φ_{11} fields by sector 3 and the $N \times N$ q_1 , \tilde{q}_1 , Φ_{12} and V_m fields by sector 4. V_m is the magnetic vector multiplet and the V_f flavor multiplet remains an undivided $N_f \times N_f$ matrix. We are here concerned only with the dependence of the scalar potential to Φ_{22} expectation value φ (our classical moduli) and the only relevant sectors are 2 and 3 where the masses will depend on φ . The sector 1 is also φ dependent but this sector is not affected by supersymmetry breaking F-terms and it remain supersymmetric, giving zero contribution to the Coleman-Weinberg potential.

Looking at the fermion masses first, the terms of the Lagrangian that give masses to fermions of sectors 2 and 3 can be written in a matrix form:

$$(\psi_{12}^\phi \quad \psi_2^{\tilde{q}} \quad \lambda_{f12}) \begin{pmatrix} 0 & h\mu & i2\varphi g_f \\ h\mu & h\varphi & -2i\mu g_f \\ -2i\varphi g_f & 2i\mu g_f & 0 \end{pmatrix} \begin{pmatrix} \psi_{21}^\phi \\ \psi_2^q \\ \lambda_{f21} \end{pmatrix} \quad (4.3)$$

The scalar masses are extracted from the F-terms and from D-terms of the flavor gauge multiplet. In the F-terms, the expectation values (4.1) preserve a mass symmetry between Φ_{12} and Φ_{21}^t and between q_2 and \tilde{q}_2^t , that allow us to write the mass matrix in a simpler 2×2 matrix.

The $W_{ab}W^{\dagger bc}$ mass matrix component is

$$\begin{pmatrix} \Phi_{12}, \Phi_{21}^t \\ q_2, \tilde{q}_2^t \end{pmatrix} \begin{pmatrix} h^2\mu^2 & h^2\mu\varphi \\ h^2\mu\varphi & h^2(\mu^2 + \varphi^2) \end{pmatrix} \quad (4.4)$$

where W_{ab} is the superpotential second derivative $\partial_a\partial_b W$ and $W_a = F_a$ is an F-term.

The $F_c W^{\dagger abc}$ mass matrix has only a $q_2\tilde{q}_2$ mass mixing component that will split the masses of scalars and pseudo-scalars. As a result, without D-term contributions, the scalar and pseudo scalar squared mass matrices are:

$$M_s^2 = h^2 \begin{pmatrix} \mu^2 & \varphi\mu \\ \varphi\mu & \varphi^2 + 2\mu^2 \end{pmatrix}, \quad M_{ps}^2 = h^2 \begin{pmatrix} \mu^2 & \varphi\mu \\ \varphi\mu & \varphi^2 \end{pmatrix} \quad (4.5)$$

with a multiplicity of $2N(N_f - N)$ real scalar fields.

Turning to the flavor D-term contribution, its mass terms are:

$$V_D \supset 2g_f^2 \text{Tr} \left[\left| \mu \left(\frac{\tilde{q}_2 - q_2^\dagger}{\sqrt{2}} \right) + \varphi \frac{\Phi_{12} - \Phi_{21}^\dagger}{\sqrt{2}} \right|^2 \right] \quad (4.6)$$

Hence, the D-term corrected scalar squared mass matrix is

$$M_s^2 = \begin{pmatrix} h^2\mu^2 + 4g_F^2\varphi^2 & \varphi\mu(h^2 - 4g_F^2) \\ \varphi\mu(h^2 - 4g_F^2) & h^2(\varphi^2 + 2\mu^2) + 4g_F^2\mu^2 \end{pmatrix} \quad (4.7)$$

Finally, by Higgs mechanism, $2N \times N_f$ vector bosons become massive, of which, N^2 have no φ dependence on their masses and $2N \times (N_f - N)$ vector bosons (multiplicity 3) get mass squared $4g_F^2(\varphi^2 + \mu^2)$.

Applying the mass values in Coleman-Weinberg expression,eq. (3.22), we get a φ dependent 1-loop correction to the classical potential. The cut-off scale Λ is set to values where the nonperturbative effects become important, the supersymmetric vacuum scale for meson fields.

4.1 Numerical Evaluation of CW Potential

Below we plot in figure 4.1 the value of φ at the minimum of the potential for continuous values of $\mathbb{R} = g_f^2/h^2$ and in figure 4.2 we plot the 1-loop potential versus φ^2/μ^2 for various values of the ratio \mathbb{R} . As we see in both plots, there is an apparent runaway at and above $\mathbb{R} = 1/2$ where also the potential meets its lowest values (figure 4.2). Logarithmic divergences in Coleman-Weinberg expression lead us to calculate the potential at higher values of φ and energy using the approach of renormalization group equations, where the runaway behavior will be clarified.

Also, the numerical analysis shows that for \mathbb{R} below 0.22, the minimum of the effective potential remains at $\varphi = 0$.

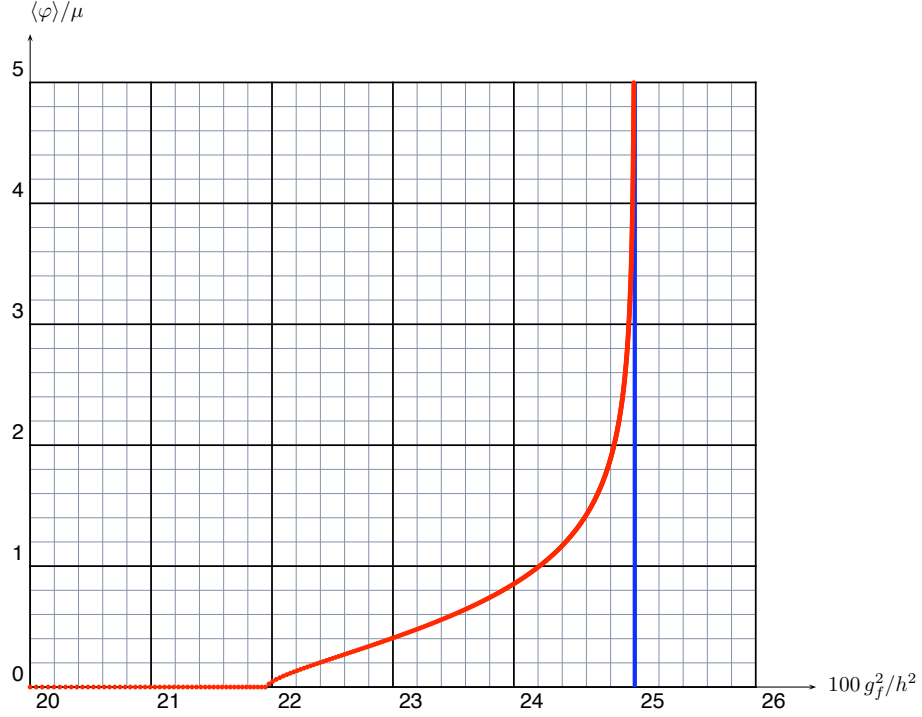


Figure 4.1: φ_{min} versus $\mathbb{R}/2 = g_f^2/2h^2$

4.2 Renormalization Group Equations

At scales much larger than μ , the supersymmetry breaking effect can be neglected and the 1-loop correction to the vacuum potential can be calculated through supersymmetric wave function renormalization.

The gauged flavor symmetry splits the flavor bifundamental Φ into a singlet and an adjoint with different wave renormalization functions. The split

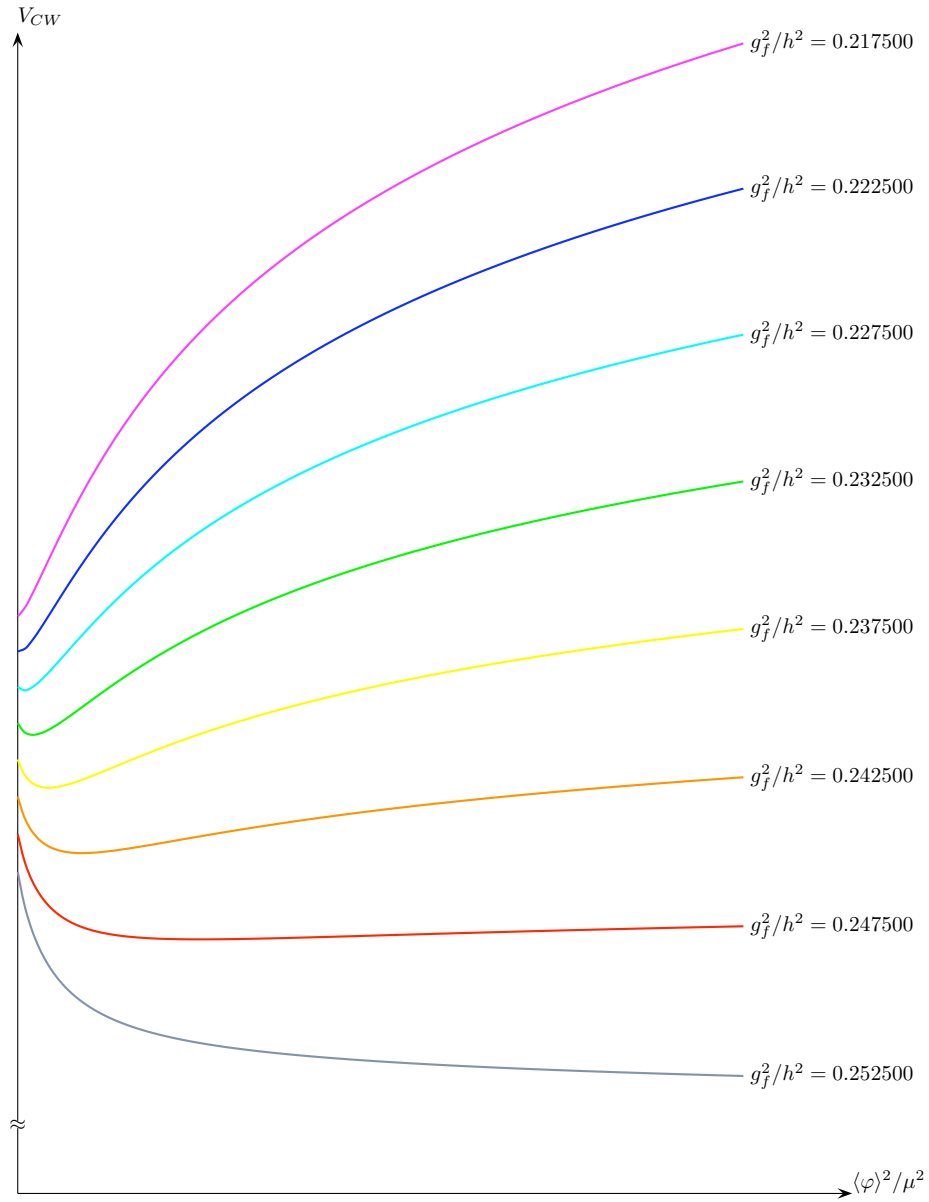


Figure 4.2: Effective potential for different values of \mathbb{R}

of the bifundamental field in the Kähler potential is

$$K = Z_1 \Phi_1 \Phi_1^\dagger + Z_{ad} \text{Tr}(\Phi_{ad} \Phi_{ad}^\dagger), \quad \text{with} \\ \Phi_1 = \frac{1}{\sqrt{N_f}} \text{Tr} \Phi \quad \text{and} \quad \Phi_{ad} = \Phi - \frac{\Phi_1}{N_f} \mathbb{I} \quad (4.8)$$

Since in (4.1) there is a single free parameter only, φ , the two wave renormalization functions will not be independent. An effective wave function is retrieved substituting (4.1) in the Kähler potential

$$K = (N_f - N) Z_{eff} \varphi^2, \quad \text{with} \quad Z_{eff} = \frac{Z_1(N_f - N) + N Z_{ad}}{N_f} \quad (4.9)$$

The tree level scalar potential (3.20) receives correction through the renormalization of the F-terms

$$V = \frac{(N_f - N) h_0^2 \mu_0^4}{Z_{eff}} \quad (4.10)$$

where h_0 and μ_0 are the unrenormalized parameters of the superpotential. The information of the wave renormalization can be encrypted in such parameters h (splits in 2) and μ :

$$h_1(E) = \frac{h_0}{Z_q(Z_1)^{1/2}}, \quad h_a(E) = \frac{h_0}{Z_q(Z_{ad})^{1/2}}, \quad \mu(E) = \mu_0 Z_q(E)^{1/2} \quad (4.11)$$

where Z_q is the wave renormalization function of q and E is the renormalization scale that is set to be equal to φ . At $E = \mu_0$ we normalize $Z_{ad} = Z_1 = Z_q = 1$.

The renormalization group equations depend on the anomalous dimension $\gamma_1, \gamma_a, \gamma_q (= \gamma_{\tilde{q}})$ of the fields Φ_1, Φ_{ad}, q and \tilde{q}

$$\gamma_1 = N \frac{h_1}{16\pi^2}, \quad \gamma_a = N \frac{h_{ad}}{16\pi^2} - N_f \frac{g_f^2}{4\pi^2}, \\ \gamma_q = \frac{h_1}{N_f 16\pi^2} + \frac{N_f^2 - 1}{N_f} \frac{h_{ad}}{16\pi^2} - \frac{g_m^2}{8\pi^2} \frac{N^2 - 1}{N} - \frac{g_f^2}{8\pi^2} \frac{N_f^2 - 1}{N_f} \quad (4.12)$$

that are used in the beta renormalization functions. We take $t(E) = \log E$ for simplification reasons.

$$\beta_1(E) = \frac{\partial h_1}{\partial t} = h_1(2\gamma_q + \gamma_1), \quad \beta_a(E) = \frac{\partial h_a}{\partial t} = h_a(2\gamma_q + \gamma_1) \quad (4.13)$$

where we will be working in the energy scale $\Lambda_f \ll \mu_0 \ll E \ll \Lambda_m$, where threshold corrections are not considered. In this regime g_f and g_m are both weak and approximately,

$$g_f^2(t) = \frac{8\pi^2}{(2N_f - N)(t - \log \Lambda_f)}, \quad g_m^2(t) = \frac{8\pi^2}{(N_f - 3N)(\log \Lambda_m - t)} \quad (4.14)$$

With this set of equations we are able to have a numerical evaluation of the potential V . We are particularly interested in knowing about the minimum of the potential. Using (4.9) and (4.10),

$$\frac{\partial V}{\partial t} \propto -(N_f - N) \frac{\partial Z_1}{\partial t} - N \frac{\partial Z_a}{\partial t} = 2(N_f - N)\gamma_1 Z_1 + 2N\gamma_a Z_a \quad (4.15)$$

Using (4.12), the condition for the potential to be at its minimum is

$$4\mathbb{R}(\varphi) = \frac{4g_f^2(\varphi)}{h_a^2(\varphi)} = 1 \quad (4.16)$$

where φ is the renormalization scale of our model.

4.3 Phase Structure

The computed condition (4.16) is only valid if the scale φ_{min} where this condition is met is within our approximation range $\mu \ll \varphi_{min} \ll \Lambda_m$. In this

case, the metastable vacuum at $\varphi = 0$ [20] slides to (4.1) with $\varphi = \varphi_{min}$, lifting the moduli space. We define a parameter τ to delineate the phase structure of our model:

$$\tau(\varphi) = \frac{\log\left(\frac{\Lambda_m}{\varphi}\right)}{\log\left(\frac{\Lambda_m}{\Lambda_f}\right)} \quad (4.17)$$

and $\tau_\mu = \tau(\mu_0)$, $\tau_{min} = \tau(\varphi_{min})$, $\tau_S = \tau(\varphi_{SUSY})$, with φ_S the expectation value of the meson fields at the supersymmetric vacuum. Naming $\nu = N_f/N$, we get from [20]

$$\varphi_S = \frac{\Lambda_m^{(\nu-3)/(\nu-1)}}{h} \mu^{2/(\nu-1)}$$

and therefore, $\tau_S = \frac{2}{(\nu-1)}\tau_\mu$. The phase structure of our model is given by:

- $\tau_{min} > \tau_\mu$: this happens when g_f is too weak, Λ_f too much below μ , such that the RG equations balance that pushing φ_{min} to lower values. But in this range $\varphi_{min} \leq \mu$ supersymmetry breaking effects must be taken in consideration and the supersymmetric RGE are not a good approximation. As a matter of fact, at this scale, with very small flavor gauge coupling, the physics works like the original ungauged ISS model, with $\varphi_{min} = 0$.
- $\tau_\mu > \tau_{min} > \frac{2}{(\nu-1)}\tau_\mu$: there is an inverse hierarchy. Metastable vacuum is shifted to φ_{min} value. The metastable vacuum has a long life, once $\varphi_S - \varphi_{min} \gg \mu$, since the bounce action will be proportional to $\left(\frac{\varphi_S - \varphi_{min}}{\mu}\right)^4$, implying in a large decay rate suppression.

- $\tau_{min} \leq \frac{2}{(\nu-1)}\tau_\mu$: the potential has a runaway behavior or it has a metastable vacuum at φ_{min} that shortly decays to the supersymmetric vacuum.

4.4 Results

Numerical evaluations of τ_{min} for several values of ν and N shows that in the general case $\tau_{min} > \tau_S$ which means that the vacuum will either stay around the same place or be shifted by inverse hierarchy, preserving the long life of the metastable vacuum.

In figure 3 below, the gray line (bottom) is the expression $2/(\nu-1)$, the blue line (middle) is τ_{min} for $N = 2$ and the violet line (top) is τ_{min} for $N = 8$. For both values of N , $\tau_{min} > 2/(\nu-1) > \tau_S$ always. Higher values for N leads to curves with higher values for τ_{min} .

Below we see an example of metastable vacuum generated far away from the origin due to inverse hierarchy. Figure 4.4(a) plots $1/\mathbb{R}$ while figure 4.4(b) plots the effective potential. We can see that the minimum of the potential is at $t \approx 4.2$ which corresponds to $1/\mathbb{R} = 4$.

In this case $\tau_{min} = 0.73$, $\tau_\mu = 0.85$ and $\tau_S = 0.73$, for $\nu = 4$ and $N = 2$.

4.5 Generic Moduli Space

As we mentioned before, the D-term equations constraint Φ_{22} into a diagonal matrix in the classical moduli space. In the general case Φ_{22} vev has

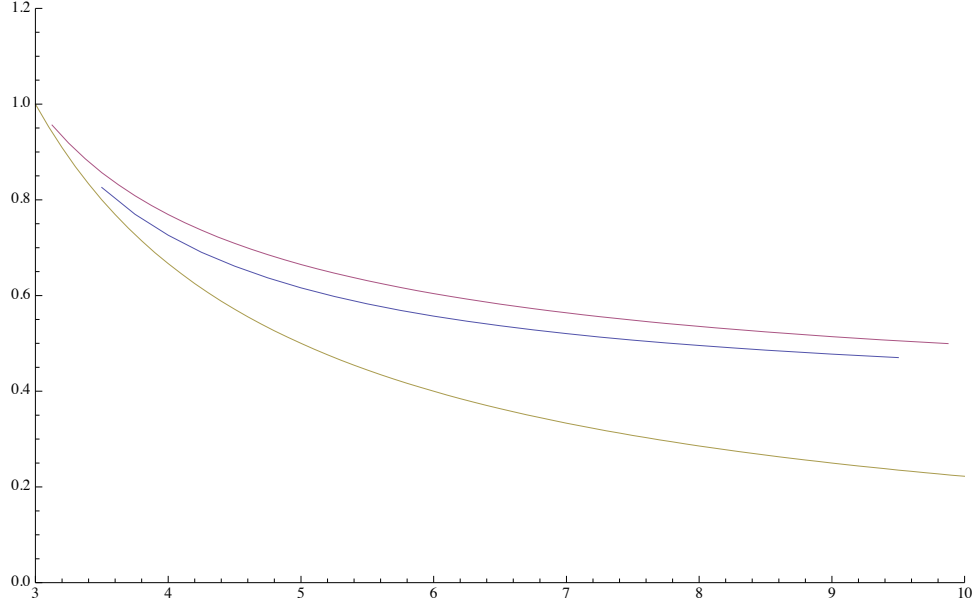
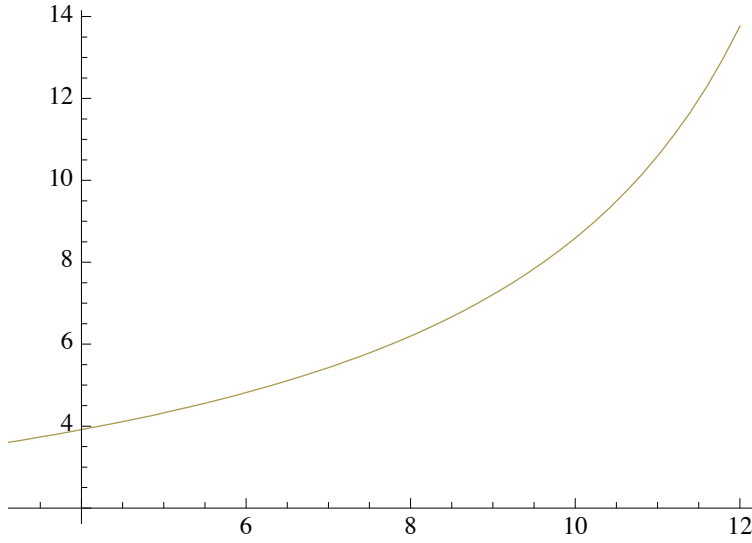
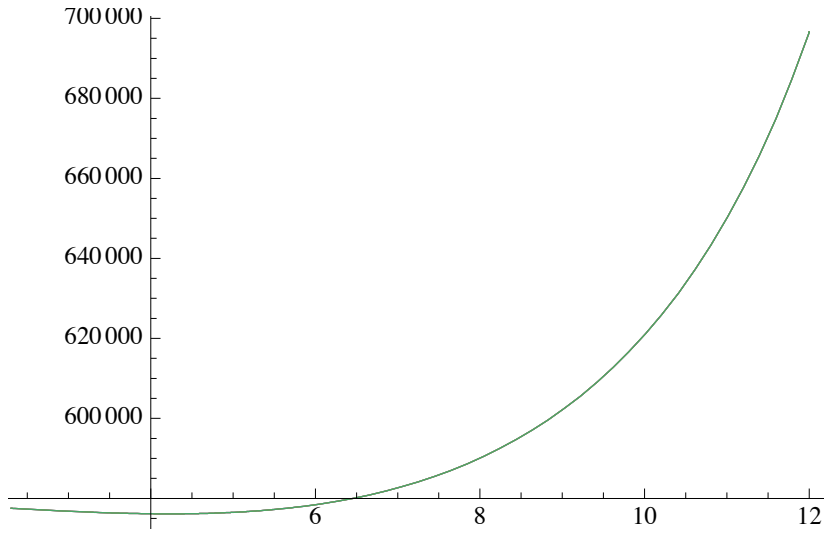


Figure 4.3: τ versus ν

different eigenvalues φ_i . In the case of $N_F - N$ distinct eigenvalues φ_i , the 1-loop potential is a sum of $N_F - N$ distinct parcels related to each eigenvalue. Each parcel may have several local minima at different values for φ_i . Therefore, the effective potential may have several meta-stable vacuum. But as we can see back in figure 4.1 and 4.2, the largest eigenvalues has the lowest minima. So the vacuum configuration where all φ_i are equal to the largest vev, φ_{max} has the lowest minimum and any other field configuration sitting in another local minimum will tunnel to the most stable meta stable vacuum, $\varphi_i = \varphi_{max}$. Therefore it suffice to study the case $\Phi_{22} = \varphi \mathbb{1}$ only.



(a) $1/\mathbb{R}$ versus $\text{Log } E$



(b) Effective Potential versus $\text{Log } E$

Figure 4.4: Minimum of potential at $\mathbb{R} = 0.25$

Chapter 5

Conclusion

Upon the end of this thesis, we would like review the goals and achievements of our work, add a few comments on our ongoing project with Vadim Kaplunovsky on metastable supersymmetry breaking [22] and trace some perspectives on the current researches on Metastable Supersymmetry Breaking (MSB).

In the present work we have explained the interest in having Supersymmetry broken only at metastable level. Phenomenologically, it save us from deal with an undetected massless R-axion, since Supersymmetry breaking mechanisms requires a spontaneous R-symmetry breaking [25] in generic models. Also, it is very easy to create MSB models. One prescription is having models with spontaneous supersymmetry breaking at the tree level, O’Raifeartaigh and Fayet-Iliopoulos models, and with approximate R-symmetry. Invariably, there will be a supersymmetric vacuum far away [21].

The model in [20] follows similar prescription, with one additional bonus. It posses a dynamical Supersymmetry restauration mechanism. Dynamical Supersymmetry restauration/breaking mechanisms together with gauge mediation are among the best alternatives to solve the hierarchy problem and

generate soft masses in the MSSM at the desirable values of $m_{soft} \sim 100\text{GeV} - 1\text{TeV}$, according to most phenomenological models [9]. Such models try to compromise the experimental constraints from the suppressed FCNC and suppressed CP violating Electric Dipole Moments in electrons and neutrons that demand soft masses and supersymmetry breaking scale to be large and the desire to have Supersymmetry breaking scale low enough to ease the hierarchy problem and contribute to gauge unification.

It is therefore important to study ISS [20] like models, that not only provide a dynamically generated intermediary scale Λ_m , but it also possesses the elements to compose the hidden sector of a gauge mediation mechanism [18] when its flavor group is gauged. In such mechanism, the secluded sector can be given by the mesons $\Phi_{ii}, N < i \leq N_f$ with non null F-terms. The messengers are generally the squarks that transform under the gauged flavor subgroup $SU(N_f - N)$ that contains the unification group.

Besides its phenomenological advantages, ISS models are very attractive for theorists too! Its SQCD like construction can be easily formulated through brane modeling in the realm of String Theory.

In this work we were able not only to show that, under reasonable assumptions of adiabatic cooling of the Universe, the Universe naturally chooses the nonsupersymmetric vacuum in the ISS model, but also, we were able to show that flavor gauged ISS models has the stability of the metastable vacuum preserved.

In a continuation of our project of investigating flavor gauged ISS models [22] two directions need to be further investigated.

First, we need to check if the nonsupersymmetric vacuum, shifted by inverse hierarchy is still favored by the adiabatic cooling of the Universe. There is a possibility that at finite temperature, a potential barrier develops between the origin in field space and the shifted nonsupersymmetric vacuum, turning the phase transition into the nonsupersymmetric configuration of the first order. If that is the case, we need to investigate such implications, although we expect that the metastable vacuum would continue to be favored by the Universe.

And second, we want to take account of the nonperturbative sector of the gauged flavor group. Such phenomena could even create singularities in the Kähler metric, generating new supersymmetric vacua closer to the metastable vacuum, endangering its long life. We will follow the work done in [24] which studies quantum mechanics effects in classical moduli in SQCD theories with adjoint fields and study dualities between distinct theories.

Metastable Supersymmetry breaking is *not* just another trend. It is here to stay, as long as Supersymmetry is a viable theory in particle physics. We hope we brought some elucidation on the subject and that our future quests in this topic and others be of interest to the scientific community. We also hope that soon the LHC may give us hints of exciting new directions in the development of theoretical particle physics, with or without SUSY!

Appendix

Appendix 1

Triangle Approximation

The decay rates of a metastable vacuum can be estimated by semiclassical techniques [10], although only a handful of potentials can have an analytical solution for the decay rates. We show here our calculation of the decay rate for an almost flat potential described in section 2.3 using the method called triangle approximation. Please refer to [15] for further details.

The triangle approximation works in cases where the potential has sharp peaks and troughs where the gradient changes sign, as in figure 1.1(a), in a theory of a single scalar field. The equation of motion will depend on the gradients of the potential

$$\lambda_{\pm} = \frac{\Delta V_{\pm}}{\Delta \phi_{\pm}}, \text{ with } \Delta V_{\pm} = (V_T - V_{\pm}) \text{ and } \phi_{\pm} = \pm(\phi_T - \phi_{\pm}) \quad (1.1)$$

The solution of the equations of motion is a bubble spherically symmetric in the four dimensional Euclidian space. Boundary conditions are established in the interior, in the surface and in the exterior of the bubble. In the interior of the bubble there is the possibility that the bubble solution is too small and the field value in the interior doesn't reach the true vacuum value ϕ_- . This will happen only for certain values of the gradient of the triangle

potential. Otherwise, the bubble will have an interior with an interior radius R_0 such that $\phi(r) = \phi_-$ for $r < R_0$.

According to such boundary conditions and gradient of the potential, Duncan and Jensen [15] were able to come with an analytical expression for the Bounce action.

In our case, we don't have just one scalar field, but many weakly coupled by the nonperturbative term. But some observations can simplify our problem.

First, we will neglect the squark contribution in the action, by substituting its expectation value in the potential, as in (2.12). Concerning the meson fields, the path in the field space from the metastable vacuum to the supersymmetric vacuum starts at the meson matrix $(\langle \Phi \rangle) = 0$ and finishes at $(\langle \Phi \rangle) = \phi_S(\mathbb{I})$. Along this path only the diagonal terms of the meson matrix will have nontrivial solution for their equation of motion. The minimization of the potential identifies the upper N diagonal terms with a single solution that we parametrize by ϕ_1 and the lower $N_f - N$ are identified to ϕ_2 , as in section 2.3.

We also observe in equation (2.13) that for small values of ϕ_2 , ϕ_2 fields (the $(N_f - N)$ bottom diagonal fields) become much lighter than the ϕ_1 fields (top N diagonal fields) of mass $\sim \mu$ and we can integrate them out. In the region where $\phi_2 \sim \phi_S$, ϕ_1 fields become light and we integrate out ϕ_2 fields. So basically our potential is separated in 2 regions, each of them with a single free parameter dependence. It is still uncertain for us how to deal with the

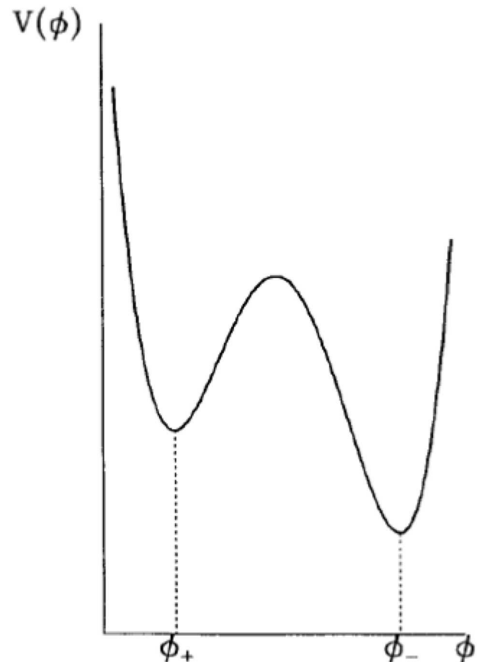
change of the number of kinetic terms in each part of the potential, but we can say that our calculation for the bounce action incorporates an error of $(N_f - N)/N$ which will not invalidate our estimatives. As mentioned in section 2.3, the triangle approximation does not work with flat potential and a little deformation is necessary.

For a potential as in figure 2.5, our gradients are

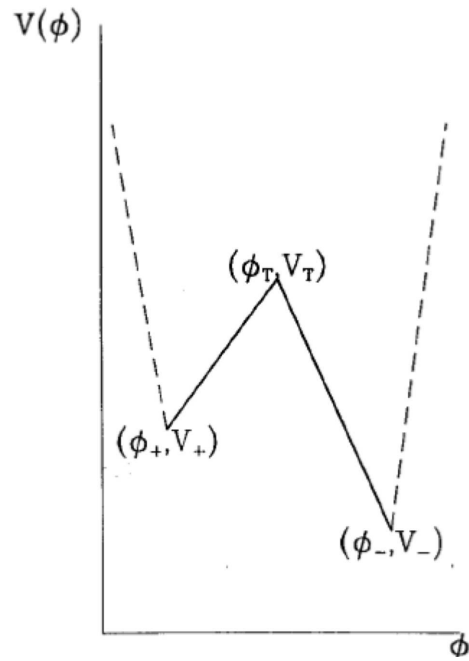
$$\lambda_- = \frac{\Delta V + \epsilon}{\phi_s} \quad , \quad \lambda_+ = \frac{\epsilon}{\phi_s} \quad \text{and} \quad c = \frac{\lambda_-}{\lambda_+} \approx \frac{\Delta V}{\epsilon} \quad (1.2)$$

Such parameters imply that the interior boundary condition for the bubble is $\phi(r) = \phi_-$ for $r < R_0$. This and the others boundary conditions gives the expression (20) in [15]. Substituting our data in the expression we obtain the ϵ independent result of equation (2.14):

$$S \approx \frac{\phi_S^4}{\Delta V} = \left[\frac{\Lambda_m}{\mu} \right]^{4(\nu-3)/(\nu-1)} h^{-6} \quad (1.3)$$



(a) Real potential with triangular shape



(b) Potential after triangle approximation

Figure 1.1: Potential before and after triangle approximation

Bibliography

- [1] Steven A. Abel, Chong-Sun Chu, Joerg Jaeckel, and Valentin V. Khoze. SUSY breaking by a metastable ground state: Why the early universe preferred the non-supersymmetric vacuum. *JHEP*, 01:089, 2007.
- [2] Steven A. Abel, Joerg Jaeckel, and Valentin V. Khoze. Naturalised supersymmetric grand unification. 2007.
- [3] Steven A. Abel and Valentin V. Khoze. Metastable SUSY breaking within the standard model. 2007.
- [4] Ian Affleck, Michael Dine, and Nathan Seiberg. Dynamical Supersymmetry Breaking in Four-Dimensions and Its Phenomenological Implications. *Nucl. Phys.*, B256:557, 1985.
- [5] Ofer Aharony and Nathan Seiberg. Naturalized and simplified gauge mediation. *JHEP*, 02:054, 2007.
- [6] Jonathan Bagger, Erich Poppitz, and Lisa Randall. The R axion from dynamical supersymmetry breaking. *Nucl. Phys.*, B426:3–18, 1994.
- [7] David Bailin and Alexander Love. *Introduction to Gauge Field Theory*. IOP, 1986.

- [8] Tom Banks and V. Kaplunovsky. NOSONOMY OF AN UPSIDE DOWN HIERARCHY MODEL. 1. *Nucl. Phys.*, B211:529, 1983.
- [9] D. J. H. Chung et al. The soft supersymmetry-breaking Lagrangian: Theory and applications. *Phys. Rept.*, 407:1–203, 2005.
- [10] Sidney R. Coleman. The Fate of the False Vacuum. 1. Semiclassical Theory. *Phys. Rev.*, D15:2929–2936, 1977.
- [11] Sidney R. Coleman and E. Weinberg. Radiative Corrections as the Origin of Spontaneous Symmetry Breaking. *Phys. Rev.*, D7:1888–1910, 1973.
- [12] Nathaniel J. Craig, Patrick J. Fox, and Jay G. Wacker. Reheating metastable O’Raifeartaigh models. *Phys. Rev.*, D75:085006, 2007.
- [13] Michael Dine and Willy Fischler. A Phenomenological Model of Particle Physics Based on Supersymmetry. *Phys. Lett.*, B110:227, 1982.
- [14] L. Dolan and R. Jackiw. Gauge invariant signal for gauge symmetry breaking. *Phys. Rev.*, D9:2904, 1974.
- [15] Malcolm J. Duncan and Lars Gerhard Jensen. Exact tunneling solutions in scalar field theory. *Phys. Lett.*, B291:109–114, 1992.
- [16] John R. Ellis, C. H. Llewellyn Smith, and Graham G. Ross. WILL THE UNIVERSE BECOME SUPERSYMMETRIC? *Phys. Lett.*, B114:227, 1982.

- [17] Willy Fischler, Vadim Kaplunovsky, Chethan Krishnan, Lorenzo Man-
nelli, and Marcus A. C. Torres. Meta-Stable Supersymmetry Breaking in
a Cooling Universe. *JHEP*, 03:107, 2007.
- [18] G. F. Giudice and R. Rattazzi. Theories with gauge-mediated supersym-
metry breaking. *Phys. Rept.*, 322:419–499, 1999.
- [19] J. Iliopoulos and B. Zumino. Broken Supergauge Symmetry and Renor-
malization. *Nucl. Phys.*, B76:310, 1974.
- [20] Kenneth Intriligator, Nathan Seiberg, and David Shih. Dynamical SUSY
breaking in meta-stable vacua. *JHEP*, 04:021, 2006.
- [21] Kenneth Intriligator, Nathan Seiberg, and David Shih. Supersymmetry
Breaking, R-Symmetry Breaking and Metastable Vacua. *JHEP*, 07:017,
2007.
- [22] Vadim Kaplunovsky and Marcus A. C. Torres. To be published.
- [23] D. A. Kirzhnits and Andrei D. Linde. A Relativistic phase transition.
Sov. Phys. JETP., 40:628, 1975.
- [24] D. Kutasov, A. Schwimmer, and N. Seiberg. Chiral Rings, Singularity
Theory and Electric-Magnetic Duality. *Nucl. Phys.*, B459:455–496, 1996.
- [25] Ann E. Nelson and Nathan Seiberg. R symmetry breaking versus super-
symmetry breaking. *Nucl. Phys.*, B416:46–62, 1994.

- [26] L. O’Raifeartaigh. Spontaneous Symmetry Breaking for Chiral Scalar Superfields. *Nucl. Phys.*, B96:331, 1975.
- [27] N. Seiberg. Electric - magnetic duality in supersymmetric nonAbelian gauge theories. *Nucl. Phys.*, B435:129–146, 1995.
- [28] Leonard Susskind. The anthropic landscape of string theory. 2003.
- [29] Steven Weinberg. Gauge and Global Symmetries at High Temperature. *Phys. Rev.*, D9:3357–3378, 1974.
- [30] Edward Witten. Mass Hierarchies in Supersymmetric Theories. *Phys. Lett.*, B105:267, 1981.
- [31] Edward Witten. Constraints on Supersymmetry Breaking. *Nucl. Phys.*, B202:253, 1982.
- [32] Fu-qiang Xu and Jin Min Yang. An Extension for Direct Gauge Mediation of Metastable Supersymmetry Breaking. 2007.

Vita

Marcus André de Carvalho Torres is a brazilian citizen born in Rio de Janeiro on December 11, 1971, son of Paulo Celso Pereira Torres, MSc., and Janilde da Graça de Carvalho Torres, MD. He received the Bachelor of Science degree in Eletrical Engineering from the Aeronautics Institute of Technology in São José dos Campos, Brazil, and was commissioned reserve Officer in Brazilian Air Force in 1994. He worked for five years in R&D and testing data communication products In the year of 2000, he enrolled in a masters program at Federal University of Rio de Janeiro (UFRJ), Brazil. He received his Master degree and enrolled at the Physics PhD program at the University of Texas at Austin in 2002. Upon receiving his PhD, he plans to join a research group at UFRJ as research fellow.

Permanent address: Rua Lopes Trovão 44 apt. 303
Niterói, RJ, Brazil 24220-071

This dissertation was typeset with L^AT_EX[†] by the author.

[†]L^AT_EX is a document preparation system developed by Leslie Lamport as a special version of Donald Knuth's T_EX Program.